Fermi National Accelerator Laboratory

FERMILAB-CONF-88/60-T
May, 1988

AN INTRODUCTION TO THE QCD PARTON MODEL[1]

R. K. Ellis
Fermi National Accelerator Laboratory
P.O. Box 500, Batavia, IL, 60510

Contents

[1] Lectures given at the 1987 Theoretical Advanced Study Institute, Santa Fe, New Mexico in July, 1987.

Operated by Universities Research Association Inc. under contract with the United States Department of Energy

1. LECTURE I

Quantum chromodynamics is the theory of interacting quarks and gluons, the constituents of the strongly interacting hadrons observed in the laboratory. These lectures will describe the way in which we can finesse our present inability to solve a strong coupling problem, namely the way in which quarks and gluons are confined in hadrons, and exploit the property of asymptotic freedom to make predictions for hadronic reactions involving large momentum transfers using weak coupling perturbation theory.

I begin with a brief description of the QCD Lagrangian and the Feynman rules which can be derived from it. This is a practical guide which does little more than introduce notation and certainly does not do justice to the elegant structure of quantum field theory. For more details I refer the reader to the standard texts[1,2]. Introductions to perturbative QCD can be found in refs. 3,4. For a more pedagogical treatment the reader is invited to consult the *TASI* lectures of earlier years[5,6].

A. Lagrangian of QCD

The Feynman rules required for a perturbative analysis of QCD can be derived from an effective Lagrange density which is given by,

$$\mathcal{L} = -\frac{1}{4}F^A_{\alpha\beta}F^{\alpha\beta}_A + \sum_{\text{flavours}} \bar{q}_a(i\hat{D} - m)_{ab}q_b + \mathcal{L}_{\text{gauge-fixing}} + \mathcal{L}_{\text{ghost}}. \tag{1.1}$$

$F^A_{\alpha\beta}$ is field strength tensor derived from the gluon field $\mathcal{A}^A_\alpha$,

$$F^A_{\alpha\beta} = \left[\partial_\alpha \mathcal{A}^A_\beta - \partial_\beta \mathcal{A}^A_\alpha - g f^{ABC}\mathcal{A}^B_\alpha \mathcal{A}^C_\beta\right] \tag{1.2}$$

and the indices A, B, C run over the eight colour degrees of freedom of the gluon field. The sum over the flavours runs over the n_f different flavours of quarks. g is the coupling constant which determines the strength of the interaction between coloured quanta. f^{ABC} are the structure constants of the $SU(3)$ colour group. The quark fields q_a are in the triplet representation of the colour group, $(a = 1,2,3)$ and D is the covariant derivative. Acting on triplet and octet fields the covariant derivative takes the form,

$$(D_\alpha)_{ab} = \partial_\alpha \delta_{ab} + ig\left(t^C \mathcal{A}^C_\alpha\right)_{ab}, \quad (D_\alpha)_{AB} = \partial_\alpha \delta_{AB} + ig(T^C \mathcal{A}^C_\alpha)_{AB} \tag{1.3}$$

t and T are matrices in the fundamental and adjoint representations of $SU(3)$ respectively,

$$\left[t^A, t^B\right] = if^{ABC}t^C, \ \left[T^A, T^B\right] = if^{ABC}T^C, \ (T^A)_{BC} = -if^{ABC}. \tag{1.4}$$

$\hat{D}$ in Eq. 1.1 is a symbolic notation for $\gamma_\mu D^\mu$ (used throughout these lectures) and the spinor indices of γ_μ and q_a have been suppressed. Otherwise we follow the notation of Bjorken and Drell[1] with metric given by $g^{\alpha\beta} = \text{diag}(1,-1,-1,-1)$ and set $\hbar = c = 1$. By convention the normalisation of the $SU(N_c)$ matrices is chosen to be,

$$\text{Tr}\, t^A t^B = T_R\, \delta^{AB}, \ T_R = \frac{1}{2}. \tag{1.5}$$

With this choice the $SU(N_c)$ colour matrices obey the following relations,

$$\sum_A t^A_{ab} t^A_{bc} = C_F\, \delta_{ac}, \ C_F = \frac{N_c^2 - 1}{2N_c}, \ N_c = 3 \tag{1.6}$$

$$\text{Tr}\, T^C T^D = \sum_{A,B} f^{ABC} f^{ABD} = N_c \delta^{CD}. \tag{1.7}$$

We cannot perform perturbation theory with the Lagrangian of Eq. 1.1 without the gauge fixing term. Indeed as we shall see below it is impossible to define the propagator for the gluon field without making a choice of gauge. The choice,

$$\mathcal{L}_{\text{gauge-fixing}} = -\frac{1}{2\,\lambda}\left(\partial^\alpha \mathcal{A}^A_\alpha\right)^2, \tag{1.8}$$

fixes the class of covariant gauges and λ is the gauge parameter. In a non-Abelian theory this covariant gauge-fixing term must be supplemented by a ghost Lagrangian, which is given by,

$$\mathcal{L}_{\text{ghost}} = \partial_\alpha \eta^{A\,\dagger}\left(D^\alpha_{AB}\eta^B\right). \tag{1.9}$$

η^A is a complex scalar field which obeys Fermi statistics. The derivation of the form of the ghost Lagrangian is best supplied by the path integral formalism[7] and the procedures due to Fadeev and Popov[8]. A simple illustration of the role played by the ghost fields, which displays the difference between Abelian and non-Abelian theories, is given in section D of this lecture. I discuss the use of axial gauges in which no ghosts are necessary in section E.

B. Feynman rules

Eqs. 1.1, 1.8 and 1.9 are sufficient to derive the Feynman rules which should be used in weak coupling perturbation theory in a covariant gauge. The Feynman rules are defined from the operator $\Phi = i\int \mathcal{L}\, d^4x$ rather than from the Lagrangian density. Φ is equal to the action multiplied by i. We can separate the effective lagrangian into a free piece $\mathcal{L}_0$, which normally contains all the terms bilinear in the fields, and an interaction piece, $\mathcal{L}_I$, which contains all the rest.

$$\begin{aligned}\Phi &= \Phi_0 + \Phi_I \\ \Phi_0 &= i\int d^4x \mathcal{L}_0(x),\ \ \Phi_I = i\int d^4x \mathcal{L}_I(x).\end{aligned} \tag{1.10}$$

The practical recipe to determine the Feynman rules is that the inverse propagator is derived from $-\Phi_0$, whereas the Feynman rules for the interacting parts of the theory which are treated as perturbations are derived from Φ_I.

This recipe (including the extra minus sign) can be understood[9] by considering the proverbial Moe and Joe who take different approaches to the quantisation of a

theory. For simplicity they consider a theory which contains only a complex scalar field ϕ and an action which contains only bilinear terms, $\Phi = \phi^* (K + K') \phi$. Moe includes both K and K' in the free Lagrangian, $\Phi_0 = \phi^* (K + K') \phi$ and using the above rule derives a propagator Δ for the ϕ field as given below. Joe treats K as the free lagrangian $\Phi_0 = \phi^* K \phi$ and regards K' as the interaction lagrangian, $\Phi_I = \phi^* K' \phi$. He includes Φ_I to all orders in perturbation theory by inserting the interaction term an infinite number of times as shown below. With the choice of signs described above they obtain the same answer for the full propagator of the ϕ field.

$$\begin{aligned} \text{Moe}: \Delta &= \frac{-1}{K + K'} \\ \text{Joe}: \Delta &= \frac{-1}{K} + \left(\frac{-1}{K}\right) K' \left(\frac{-1}{K}\right) + \left(\frac{-1}{K}\right) K' \left(\frac{-1}{K}\right) K' \left(\frac{-1}{K}\right) + \cdots = \frac{-1}{K + K'} \end{aligned} \tag{1.11}$$

This demonstrates the internal consistency of the recipe.

Thus for example the inverse fermion propagator can be obtained by making the identification $\partial^\alpha = -ip^\alpha$ for an incoming field. The two point function of the quark field becomes,

$$\Gamma^{(2)}_{ab}(p) = -i\delta_{ab} (\hat{p} - m) \tag{1.12}$$

which is the inverse of the propagator given in Table 1. Similarly the inverse propagator of the gluon field is found to be,

$$\Gamma^{(2)}_{\{AB,\,\alpha\beta\}}(p) = i\delta_{AB} \left[p^2 g_{\alpha\beta} - (1 - \frac{1}{\lambda}) p_\alpha p_\beta\right]. \tag{1.13}$$

It is easy to check that without the gauge fixing term this function would have no inverse. The result for the gluon propagator Δ is as given in Table 1.

$$\Gamma^{(2)}_{\{AB,\,\alpha\beta\}}(p)\ \Delta^{(2)}_{\{BC,\,\beta\gamma\}}(p) = \delta_{AC} g_{\alpha\gamma} \tag{1.14}$$

$$\Delta^{(2)}_{\{BC,\,\beta\gamma\}}(p) = \delta_{BC} \frac{i}{p^2} \left[-g_{\beta\gamma} + (1 - \lambda) \frac{p_\beta p_\gamma}{p^2}\right]. \tag{1.15}$$

Replacing derivatives with the appropriate momenta, Eqs. 1.1, 1.8 and 1.9 can be used to derive all the rules in Table 1.

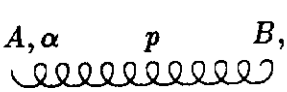

$$\delta^{AB}\left[-g^{\alpha\beta}+(1-\lambda)\frac{p^\alpha p^\beta}{p^2+i\epsilon}\right]\frac{i}{p^2+i\epsilon}$$

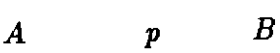

$$\delta^{AB}\frac{i}{p^2+i\epsilon}$$

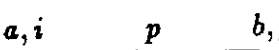

$$\delta^{ab}\frac{i}{(\hat{p}-m+i\epsilon)_{ji}}$$

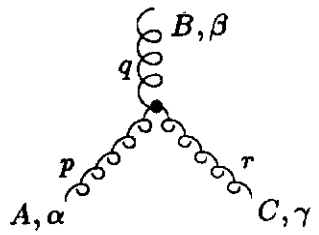

$$-gf^{ABC}\left[g^{\alpha\beta}(p-q)^\gamma+g^{\beta\gamma}(q-r)^\alpha+g^{\gamma\alpha}(r-p)^\beta\right]$$

(all momenta incoming)

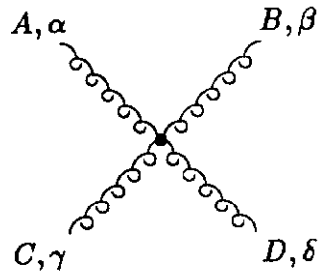

$$-ig^2f^{XAC}f^{XBD}(g_{\alpha\beta}g_{\gamma\delta}-g_{\alpha\delta}g_{\beta\gamma})$$
$$-ig^2f^{XAD}f^{XBC}(g_{\alpha\beta}g_{\gamma\delta}-g_{\alpha\gamma}g_{\beta\delta})$$
$$-ig^2f^{XAB}f^{XCD}(g_{\alpha\gamma}g_{\beta\delta}-g_{\alpha\delta}g_{\beta\gamma})$$

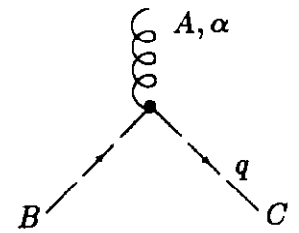

$$gf^{ABC}q^\alpha$$

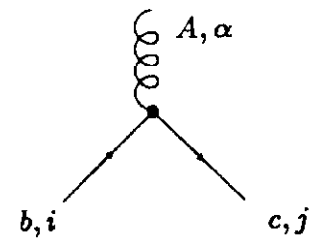

$$-ig\left(t^A\right)_{cb}(\gamma^\alpha)_{ji}$$

Table 1: Feynman rules for QCD

C. Renormalisation

When the Feynman rules specified above are used to calculate loop diagrams ultraviolet divergences are encountered. Because of the renormalisability of QCD all such divergences can be absorbed order by order in perturbation theory by defining renormalised couplings, masses and fields[10]. The Lagrangian introduced in the previous sections is therefore the bare Lagrangian which depends on the bare parameters and fields which we now denote by the suffix 0.

The renormalised Lagrangian is obtained by rewriting Eq. 1.1 in terms of renormalised fields,

$$\mathcal{L}(\mathcal{A}_0^\alpha, q_0, \eta_0, m_0, g_0, \lambda_0) = \mathcal{L}(\mathcal{A}^\alpha, q, \eta, m, g\mu^\epsilon, \lambda) + \delta\mathcal{L}(\mathcal{A}^\alpha, q, \eta, m, g\mu^\epsilon, \lambda) \quad (1.16)$$

Once we specify the relationship between bare and renormalised quantities, Eq. 1.16 defines the counterterms $\delta\mathcal{L}$. Eq. 1.16 assumes that the loop integrals are regularised by continuing the dimension of space-time to $d = 4 - 2\epsilon$ dimensions. More information on this procedure is given below. A mass scale μ has been introduced to keep the coupling constant dimensionless in d dimensions. The advantage of working with renormalised fields is that the Greens functions of the theory have a smooth limit as the cut-off is removed in terms of renormalised fields. The bare and renormalised quantities are related by,

$$\mathcal{A}^a = Z_3^{-\frac{1}{2}}\mathcal{A}_0^a, \quad \lambda = \frac{\lambda_0}{Z_3}, \quad q = Z_2^{-\frac{1}{2}}q_0, \quad \eta = \tilde{Z}_3^{-\frac{1}{2}}\eta_0, \quad m_0 = mZ_m$$

$$g_0 = g\mu^\epsilon \frac{Z_1}{Z_3^{\frac{3}{2}}} = g\mu^\epsilon \frac{\tilde{Z}_1}{\tilde{Z}_3 Z_3^{\frac{1}{2}}} = g\mu^\epsilon \frac{Z_1^F}{Z_2 Z_3^{\frac{1}{2}}} = g\mu^\epsilon \frac{Z_4^{\frac{1}{2}}}{Z_3} \quad (1.17)$$

Note that the renormalisation constants of the theory satisfy the Ward identities,

$$Z_1/Z_3 = \tilde{Z}_1/\tilde{Z}_3 = Z_1^F/Z_2 = Z_4/Z_1 \quad (1.18)$$

which ensure the universality of charge renormalisation. These are the generalisation to non-Abelian theory of the QED relation, $Z_1 = Z_2$. Because of the renormalisability of the theory all matrix elements calculated with $\mathcal{L} + \delta\mathcal{L}$ are finite. We write

$$\mathcal{L} + \delta\mathcal{L} = -\frac{1}{4}Z_3\left(\partial_\alpha\mathcal{A}_\beta^B - \partial_\beta\mathcal{A}_\alpha^B\right)^2 - \frac{1}{2\lambda}(\partial_\alpha\mathcal{A}_\beta^B)^2 + Z_2^F\bar{q}_a(i\hat{\partial} - Z_m m)q_a + \tilde{Z}_3\partial_\alpha\eta_B^\dagger\partial^\alpha\eta_B$$

$$+\frac{g}{2}\mu^{\epsilon}Z_1 f^{ABC}(\partial_\alpha \mathcal{A}^A_\beta - \partial_\beta \mathcal{A}^A_\alpha)\mathcal{A}^B_\alpha \mathcal{A}^C_\beta + \tilde{Z}_1 ig\mu^{\epsilon}\partial_\alpha \eta^\dagger_B (T\cdot\mathcal{A}^\alpha)_{BC}\eta_C - Z^F_1 g\mu^{\epsilon}\bar{q}_a(t\cdot\hat{A})_{ab}q_b$$

$$-\frac{g^2}{4}\mu^{2\epsilon}Z_4 f^{ABC}f^{ADE}\mathcal{A}^B_\alpha \mathcal{A}^C_\beta \mathcal{A}^D_\alpha \mathcal{A}^E_\beta. \qquad (1.19)$$

Thus the counterterms are given by,

$$\delta\mathcal{L} = -\frac{1}{4}(Z_3-1)\left(\partial_\alpha \mathcal{A}^B_\beta - \partial_\beta \mathcal{A}^B_\alpha\right)^2$$

$$+i(Z^F_2-1)\bar{q}_a\hat{\partial}q_a - (Z^F_2 Z_m - 1)\bar{q}_a m q_a + (\tilde{Z}_3-1)\partial_\alpha\eta^\dagger_B\partial^\alpha\eta_B$$

$$+\frac{g}{2}\mu^{\epsilon}(Z_1-1)f^{ABC}(\partial_\alpha \mathcal{A}^B_\beta - \partial_\beta \mathcal{A}^A_\alpha)\mathcal{A}^B_\alpha \mathcal{A}^C_\beta + (\tilde{Z}_1-1)ig\mu^{\epsilon}\partial_\alpha\eta^\dagger_B(T\cdot\mathcal{A}^\alpha)_{BC}\eta_C$$

$$-(Z^F_1-1)g\mu^{\epsilon}\bar{q}_a(t\cdot\hat{A})_{ab}q_b - \frac{g^2}{4}\mu^{2\epsilon}(Z_4-1)f^{ABC}f^{ADE}\mathcal{A}^B_\alpha\mathcal{A}^C_\beta\mathcal{A}^D_\alpha\mathcal{A}^E_\beta. \qquad (1.20)$$

The Z's are defined order by order in perturbation theory to cancel all the ultraviolet divergences. In the intermediate stages of the calculation we must introduce some regularisation procedure to control these divergences. The most effective regulator is the method of dimensional regularisation which continues the dimension of space-time to $d = 4-2\epsilon$ dimensions[11]. This method of regularisation has the advantage that the Ward Identities of the theory are preserved at all stages of the calculation. Integrals over loop momenta are performed in d dimensions with the help of the following formula,

$$\int \frac{d^dk}{(2\pi)^d}\frac{(-k^2)^r}{\left[-k^2+C-i\varepsilon\right]^m} = \frac{i(4\pi)^{\epsilon}}{16\pi^2}\left[C-i\varepsilon\right]^{2+r-m-\epsilon}\frac{\Gamma(r+d/2)}{\Gamma(d/2)}\frac{\Gamma(m-r-2+\epsilon)}{\Gamma(m)}. \qquad (1.21)$$

To demonstrate Eq. 1.21, we first perform a Wick rotation of the k_0 contour anti-clockwise. This is dictated by the $i\varepsilon$ prescription, since for real C the poles coming from the denominator of Eq.1.21 lie in the second and fourth quadrant of the k_0 complex plane. Thus by anti-clockwise rotation we encounter no poles. After rotation by an angle $\pi/2$, the k_0 integral runs along the imaginary axis in the k_0 plane, $(-i\infty < k_0 < i\infty)$. In order to deal only with real quantities we make the substitution $k_0 = i\kappa_d, k_j = \kappa_j$ for all $j \neq 0$ and introduce $|\kappa| = \sqrt{\kappa_1^2+\kappa_2^2\ldots+\kappa_d^2}$. We obtain a d-dimensional Euclidean integral which may be written as,

$$\int d^d\kappa\, f(\kappa^2) = \int d|\kappa|\, f(\kappa^2)\,|\kappa|^{d-1}\sin^{d-2}\theta_{d-1}\sin^{d-3}\theta_{d-2}\ldots$$
$$\times \sin\theta_2\, d\theta_{d-1}d\theta_{d-2}\ldots d\theta_2 d\theta_1. \qquad (1.22)$$

The range of the angular integrals is $0 \leq \theta_i \leq \pi$ except for $0 \leq \theta_1 \leq 2\pi$. The angular integrations, which only give an overall factor, can be performed using

$$\int_0^\pi d\theta \ \sin^d\theta = \sqrt{\pi}\frac{\Gamma\left(\frac{(d+1)}{2}\right)}{\Gamma\left(\frac{(d+2)}{2}\right)}. \tag{1.23}$$

We therefore find that the left hand side of Eq. 1.21 can be written as,

$$\frac{2i}{(4\pi)^{d/2}\Gamma\left(d/2\right)}\int_0^\infty d|\kappa| \ \frac{|\kappa|^{d+2r-1}}{\left[\kappa^2+C\right]^m}. \tag{1.24}$$

This last integral can be reduced to a Beta function,

$$\int_0^\infty dx \frac{x^s}{\left[x^2+C\right]^m} = \frac{\Gamma\left(\frac{(s+1)}{2}\right)}{2}\frac{\Gamma\left(m-s/2-1/2\right)}{\Gamma\left(m\right)}C^{s/2+1/2-m} \tag{1.25}$$

which demonstrates Eq. 1.21.

When calculating the two, three and four point functions of the quark, gluon and ghost fields the ultraviolet divergences of the theory appear as poles in ϵ. In the mimimal subtraction (MS) renormalisation scheme[9] one chooses the various Z's of the theory in such a way that the poles are all cancelled. In one loop this leads to the renormalisation constants given in Table 2. Note that the renormalisation constants depend on the gauge parameter. The scheme is called minimal because the renormalisation constants of the theory contain only the pole parts.

D. The physical motivation for ghosts

I now provide a heuristic argument, due to Feynman[12], for the presence of the ghost term in the Lagrangian. The argument considers the consequences of unitarity for processes involving gluons. One of the simplest examples is the reaction in which a quark and an antiquark annihilate to produce a pair of gluons,

$$q(p) + \bar{q}(p') \rightarrow g(q) + g(q') \tag{1.26}$$

The momenta carried by the various fields are shown in brackets. For simplicity we consider massless quark fields. The three diagrams which contribute in lowest

Z_3	$1+\frac{g^2}{16\pi^2}\frac{1}{\epsilon}\Big[N_c(\frac{13}{6}-\frac{\lambda}{2})-\frac{4}{3}n_f T_R\Big]$
Z_1	$1+\frac{g^2}{16\pi^2}\frac{1}{\epsilon}\Big[N_c(\frac{17}{12}-\frac{3\lambda}{4})-\frac{4}{3}n_f T_R\Big]$
Z_4	$1+\frac{g^2}{16\pi^2}\frac{1}{\epsilon}\Big[N_c(\frac{2}{3}-\lambda)-\frac{4}{3}n_f T_R\Big]$
$\tilde{Z}_3$	$1+\frac{g^2}{16\pi^2}\frac{1}{\epsilon}\Big[N_c(\frac{3}{4}-\frac{\lambda}{4})\Big]$
$\tilde{Z}_1$	$1-\frac{g^2}{16\pi^2}\frac{1}{\epsilon}\Big[N_c\frac{\lambda}{2}\Big]$
Z_2^F	$1-\frac{g^2}{16\pi^2}\frac{1}{\epsilon}\Big[C_F\lambda\Big]$
Z_1^F	$1-\frac{g^2}{16\pi^2}\frac{1}{\epsilon}\Big[N_c(\frac{3}{4}+\frac{\lambda}{4})+C_F\lambda\Big]$
Z_g	$1-\frac{g^2}{16\pi^2}\frac{1}{\epsilon}\Big[N_c\frac{11}{6}-n_f T_R\frac{2}{3}\Big]$

Table 2: Minimal subtraction renormalisation constants in a general covariant gauge at one loop order.

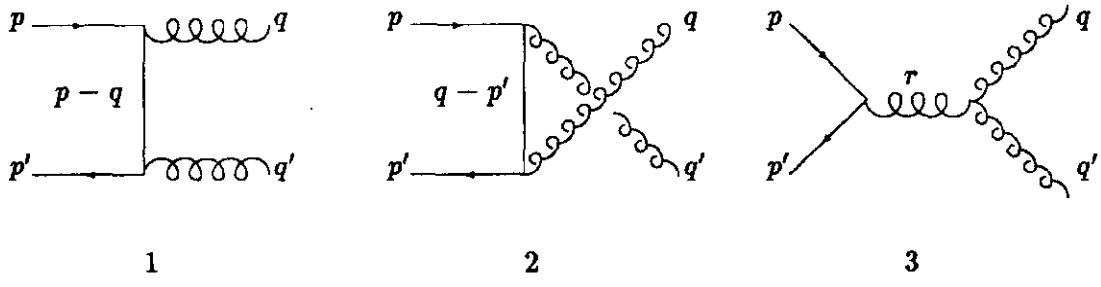

Figure 1: Feynman Diagrams for $q\overline{q} \to gg$

order are shown in Fig. 1. Using the Feynman rules of Table 1, and choosing the Feynman gauge $\lambda = 1$, the three diagrams may be written as,

$$\begin{aligned}
M_1^{\alpha\beta} &= -ig^2\, \bar{v}(p')\, \gamma^\beta t^B \frac{1}{(\hat{p}-\hat{q})} \gamma^\alpha t^A\, u(p), \\
M_2^{\alpha\beta} &= -ig^2\, \bar{v}(p')\, \gamma^\alpha t^A \frac{1}{(\hat{q}-\hat{p}')} \gamma^\beta t^B\, u(p), \\
M_3^{\alpha\beta} &= (-ig)\Big(-gf^{ABC} V^{\alpha\beta\gamma}(-q,-q',r)\Big)\Big(-\frac{ig_{\gamma\delta}}{r^2}\Big)\, \bar{v}(p')\, \gamma^\delta t^C\, u(p) \\
&= -ig^2\, V^{\alpha\beta\gamma}(-q,-q',r)\, \frac{1}{r^2}\, \bar{v}(p')\gamma_\gamma \Big[t^A, t^B\Big] u(p). \qquad (1.27)
\end{aligned}$$

α and β (A and B) are the Lorentz indices (colour indices) of the lines with momenta q and q' respectively. The momentum structure of the three gluon vertex is represented by,

$$V^{\alpha\beta\gamma}(-q,-q',r) = \Big[g^{\alpha\beta}(q'-q)^\gamma - g^{\beta\gamma}(q'+r)^\alpha + g^{\gamma\alpha}(r+q)^\beta\Big] \qquad (1.28)$$

and the momentum $r = p + p' = q + q'$. The full amplitude is given by the sum of the three diagrams,

$$M^{\alpha\beta} = M_1^{\alpha\beta} + M_2^{\alpha\beta} + M_3^{\alpha\beta}. \qquad (1.29)$$

In order to calculate the transition probability T for this process we must square the amplitude and sum over the physical polarisations ϵ and ϵ' of the two gluons with momenta q and q'. If the colours of the gluons are not observed we should sum over them also. For a real physical gluon there are two polarisations which

we denote by the label l, $(l = 1, 2)$. The square of the amplitude is

$$T = \sum_{\text{polarisations}} M^{\dagger\alpha'\beta'} \epsilon^*_{\alpha'}(l) \epsilon'^*_{\beta'}(l') \, M^{\alpha\beta} \epsilon_\alpha(l) \epsilon'_\beta(l'). \tag{1.30}$$

The normal method of performing the polarisation sum in QED is to use the equation,

$$\sum_l \epsilon^{*\alpha'}(l) \epsilon^\alpha(l) = -g^{\alpha'\alpha} \tag{1.31}$$

The derivation of Eq. 1.31 is as follows. A free wave must satisfy Maxwell's equation, $\partial^\alpha(\partial_\alpha A_\beta - \partial_\beta A_\alpha) = 0$ which in momentum space implies that,

$$q^2 \epsilon^\beta - q^\beta \epsilon \cdot q = 0. \tag{1.32}$$

Since for a real gluon $q^2 = 0$, we conclude from Eq. 1.32 that $\epsilon \cdot q = 0$. Let us choose a specific frame for the momenta q and q'. In the centre of momentum frame for the two outgoing gluons the components of q may be written, $q = (q_0, q_1, q_2, q_3)$

$$q = \frac{\sqrt{s}}{2}(1, 0, 0, 1), \quad q' = \frac{\sqrt{s}}{2}(1, 0, 0, -1). \tag{1.33}$$

In addition we shall make a gauge choice for the real gluons $\mathcal{A}^0 = 0$. The two polarisations of the gluon with momentum q which satisfy the above constraints are,

$$\epsilon(1) = (0, 1, 0, 0), \quad \epsilon(2) = (0, 0, 1, 0). \tag{1.34}$$

In the frame given by Eq. 1.33 the polarisations ϵ' can be similarly chosen. We may therefore write the sum over polarisations as,

$$\sum_l \epsilon^{*\alpha'}(l) \epsilon^\alpha(l) = -g^{\alpha'\alpha} + g^{00} - g^{33} = \left(-g^{\alpha'\alpha} + \frac{q'^{\alpha'} q^\alpha + q^{\alpha'} q'^{\alpha}}{(q \cdot q')} \right). \tag{1.35}$$

Eq. 1.35 contains extra terms not present in Eq. 1.31. In QED the extra terms proportional to q and q' make no contribution because it can be shown that,

$$q^\alpha M_{\alpha\beta} = q^\alpha M^\dagger_{\alpha\beta} = 0. \tag{1.36}$$

This can be viewed as a consequence of electromagnetic gauge invariance,

$$\mathcal{A}^\alpha \to \mathcal{A}^\alpha + \partial^\alpha \Lambda, \quad \epsilon^\alpha \to \epsilon^\alpha + \lambda q^\alpha. \tag{1.37}$$

Note however that the gauge invariance of the theory has been broken by the introduction of the gauge fixing term. In addition in a non-Abelian theory the behaviour of the gauge field under a gauge transformation is more complicated than Eq. 1.37. We shall therefore explicitly study whether the vestiges of gauge symmetry are sufficient to ensure that $q_\alpha M^{\alpha\beta} = 0$ in a non-Abelian theory.

We contract each of the three graphs in Fig. 1 with q_α. From Eq. 1.27 the first two graphs give,

$$\left.\begin{aligned} q_\alpha M_1^{\alpha\beta} &= ig^2\,\bar{v}(p')\,\gamma^\beta t^B t^A\,u(p) \\ q_\alpha M_2^{\alpha\beta} &= -ig^2\,\bar{v}(p')\,\gamma^\beta t^A t^B\,u(p) \end{aligned}\right\} = -ig^2\,\bar{v}(p')\,\gamma^\beta\left[t^A,t^B\right]u(p) \qquad (1.38)$$

In order to calculate $q_\alpha M_3^{\alpha\beta}$ it is useful to first prove a subsidiary result. We have

$$\begin{aligned} q_\alpha V^{\alpha\beta\gamma}(-q,-q',r) &= q^\beta(q'-q)^\gamma + g^{\beta\gamma}(q'^2 - r^2) + q^\gamma(r+q)^\beta \\ &\equiv (g^{\beta\gamma}q'^2 - q'^\beta q'^\gamma) - (g^{\beta\gamma}r^2 - r^\beta r^\gamma). \end{aligned} \qquad (1.39)$$

Using this result to calculate $q_\alpha M_3^{\alpha\beta}$ we denote the four terms coming from the last line of Eq. 1.39 as $(a),(b),(c)$ and (d). These four contributions are,

$$\begin{aligned} (a)\ q_\alpha M_3^{\alpha\beta} &= 0, \quad q'^2 = 0 \\ (b)\ q_\alpha M_3^{\alpha\beta} &= +ig^2\left(\frac{1}{r^2}\right)\bar{v}(p')\,\hat{q}'\left[t^A,t^B\right]u(p)\,q'^\beta = H(q')q'^\beta \\ (c)\ q_\alpha M_3^{\alpha\beta} &= +ig^2\,\bar{v}(p')\,\gamma^\beta\left[t^A,t^B\right]u(p) \\ (d)\ q_\alpha M_3^{\alpha\beta} &= -ig^2\,\bar{v}(p')\,\hat{r}\left[t^A,t^B\right]u(p)\,\frac{r^\beta}{r^2} = 0. \end{aligned} \qquad (1.40)$$

Contribution (a) vanishes for an on-shell gluon. Contibution (c) cancels the contribution of the other two diagrams, Eq. 1.38. Contribution (d) vanishes by the equation of motion for massless quarks.

$$\bar{v}(p')\,\hat{r}\,u(p) = \bar{v}(p')\,\hat{p}\,u(p) + \bar{v}(p')\,\hat{p}'\,u(p) = 0. \qquad (1.41)$$

Adding the contributions of all three diagrams we obtain,

$$q_\alpha\left(M_1^{\alpha\beta} + M_2^{\alpha\beta} + M_3^{\alpha\beta}\right) = q_\alpha M^{\alpha\beta} = H(q')q'^\beta \qquad (1.42)$$

where H is defined to be

$$H(q') = ig^2\Big(\frac{1}{r^2}\Big)\bar{v}(p')\ \hat{q}'\Big[t^A, t^B\Big]\ u(p). \tag{1.43}$$

The conclusion is that in general $q_\alpha M^{\alpha\beta} \neq 0$. Note that if the other gluon with momentum q' is a free physical source, it will satisfy $\epsilon'(l') \cdot q' = 0$. Only in this case will the result of contracting with q^α give zero.

$$q_\alpha M^{\alpha\beta}\epsilon'_\beta(l') = 0. \tag{1.44}$$

By Bose symmetry we obtain the result of contraction with q'_β,

$$q'_\beta M^{\alpha\beta} = -H(q)q^\alpha \tag{1.45}$$

where the minus sign comes from the colour commutator in Eq. 1.43. Because Eq. 1.44 gives zero only for a free physical source it is not permitted to use Eq. 1.31 to sum over physical polarisations in a non-Abelian theory. The extra terms in Eq. 1.35 do not cancel. The correct result for the transition probability is obtained by explicitly summing over the transverse degrees of freedom.

$$\begin{aligned} T &= \sum_{\text{polarisations}} M^{\dagger\,\alpha'\beta'}\epsilon^*_{\alpha'}(l)\epsilon'^*_{\beta'}(l')M^{\alpha\beta}\epsilon_\alpha(l)\epsilon'_\beta(l') \\ &= M^{\dagger\alpha'\beta'}M^{\alpha\beta}\left(-g_{\alpha\alpha'} + \frac{(q_\alpha q'_{\alpha'} + q_{\alpha'}q'_\alpha)}{q\cdot q'}\right)\left(-g_{\beta\beta'} + \frac{q_\beta q'_{\beta'} + q_{\beta'}q'_\beta}{q\cdot q'}\right) \\ &\equiv \sum_{\alpha,\beta} M^\dagger_{\alpha\beta}M^{\alpha\beta} + H^\dagger(q')H(q) + H^\dagger(q)H(q'). \end{aligned} \tag{1.46}$$

The first term in Eq. 1.46 is the result which would have been obtained using Eq. 1.31. The additional terms are required in a non-Abelian theory to subtract unphysical polarisations which have been included in the first term. Note that the function H is proportional to the commutator of two $SU(3)$ matrices and hence would not be present in an Abelian theory.

We shall now show that the extra terms in Eq. 1.46 are exactly what one would obtain from ghost loops taking the discontinuity of the amplitude $q\bar{q} \to q\bar{q}$. In the Feynman gauge the contribution of the diagrams with gluon exchange to the g^4 amplitude $q\bar{q} \to q\bar{q}$ is,

$$\sum_{\alpha,\beta}\frac{1}{2}M_{\alpha\beta}(-q,-q',r)M^{\alpha\beta}(q,q',-r) \times \text{ gluon propagator pieces } . \tag{1.47}$$

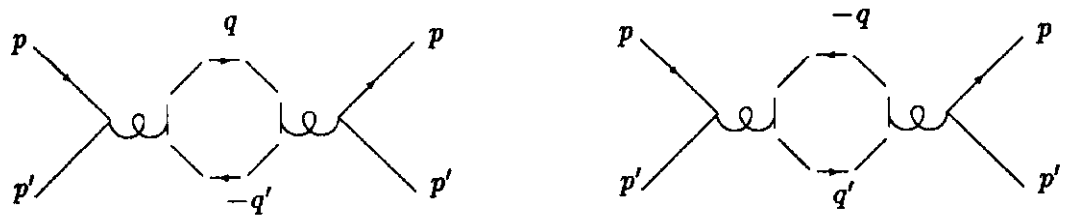

Figure 2: Feynman Diagrams for $q\bar{q} \to q\bar{q}$ with ghost loops

The diagrams included in Eq. 1.47 are the box and triangle diagrams and self energy diagrams involving gluons. They are in one-to-two correspondence with the square of the diagrams in Fig. 1. In order to make the correspondence with the real diagrams more apparent we rewrite this as

$$-\frac{1}{2}\sum_{\alpha,\beta} M^{\dagger}_{\alpha\beta}(-q,-q',r)M^{\alpha\beta}(-q,-q',r) \times \text{ gluon propagator pieces.} \quad (1.48)$$

The Feynman rules require that the ghost diagrams shown in Fig. 2 must also be included. The contribution of diagram (g_1) is

$$(-1)\, g^4 f^{CAB} f^{ABD} \bar{v}(p')\, \hat{q}\, t^C\, u(p) \left(-\frac{i}{r^2}\right) \bar{u}(p)\, \hat{q}'\, t^D\, v(p') \left(-\frac{i}{r^2}\right) \equiv -H(q)H^{\dagger}(q') \quad (1.49)$$

An extra minus sign must be included for the ghost loop because the ghost field obeys Fermi statistics. The minus sign for the ghost loop is shown explicitly in Eq. 1.49. Diagram (g_2) can be similarly calculated. Adding all the terms up we obtain the full result for the process $q + \overline{q} \to q + \overline{q}$

$$-\frac{1}{2}\int \frac{d^4q}{(2\pi)^4}\frac{d^4q'}{(2\pi)^4}(2\pi)^4\delta^4(r-q-q')\frac{1}{(q^2+i\varepsilon)(q'^2+i\varepsilon)}$$
$$\left[\sum M^{\dagger}_{\alpha\beta}(-q,-q',r)M^{\alpha\beta}(-q,-q',r) + H^{\dagger}(q')H(q) + H^{\dagger}(q)H(q')\right] \quad (1.50)$$

The s-channel discontinuity of this diagram is obtained using the Cutkosky rules[13]. The discontinuity is obtained by making the replacement $1/(q^2+i\varepsilon) \to -2i\pi\delta(q^2)$

for the propagators. Up to overall factors associated with the real phase space integrals which have not been included, the discontinuity of Eq. 1.50 agrees with Eq. 1.46 and the unitarity of the theory is confirmed.

The factors of one half which have appeared in Eqs. 1.47, 1.48 and 1.50 require some explanation. For the virtual process $q\bar{q} \to q\bar{q}$ these are the statistical factors which occur because the gluons circulating in the loop are identical. They are included for the ghost diagrams also, because diagrams (g_1) and (g_2) are not normally counted as separate diagrams. In fact, after integration over the ghost loop, the contributions of (g_1) and (g_2) are identical. One therefore has the option of either including both diagrams with a factor of one half, or of including only one diagram. For the total rate for real gluon emission derived from Eq. 1.46 the same statistical factor is also needed. It ensures that the phase space of the identical particles is integrated over only once.

We therefore conclude from this simple example that the role played by the ghost loops is to restore unitarity by removing unphysical polarisations. Were it not for the presence of the ghost loops, the s-channel discontinuity of the two gluon mediated forward amplitude $q\bar{q} \to q\bar{q}$ would not agree with the transition probability for the physical process $q\bar{q} \to gg$ summed over the two physical polarisations of the gluons.

This example does not demonstrate that the inclusion of ghost diagrams works to all orders in perturbation theory. The ghost diagrams are required only in internal loops and are not free physical states. Note however that it is sometimes convenient to turn the above argument around and use ghost diagrams to sum over physical polarisations. The reason for this is the following. Let us suppose we are calculating a process in which l external gluons are emitted. In order to sum over physical polarisations we must contract the indices of $l-1$ of them with the generalisation of Eq. 1.35. This multiplies the number of terms in the matrix element squared by 3^{l-1}. It may therefore be more efficient to perform the polarisation sum using Eq. 1.31, but include ghost loops to cancel the extra terms which Eq. 1.31 erroneously introduces. The extra terms in Eq. 1.35, not present in Eq. 1.31 also cancel unphysical polarisations, but using ghost loops leads to a smaller number of terms. This is because the information contained in the Ward identity has already been included.

For completeness we quote the final answer for $q\bar{q} \to gg$ summed over initial and final colours and spins.

$$\sum |M|^2 = g^4 \frac{2(N_c^2-1)}{N_c} \left(\frac{(N_c^2-1)}{ut} - \frac{2N_c^2}{s^2} \right) (u^2+t^2), \quad N_c = 3 \qquad (1.51)$$

where $s = (p+p')^2$, $t = (p-q)^2$, $u = (p'-q')^2$. The transition probability for the process $qg \to qg$ is obtainable from Eq. 1.51 by crossing.

E. Physical gauges

In the previous subsection we investigated some of the complications which occur in the covariant gauges, by using the explicit example of the Feynman gauge. This is because use of the Feynman gauge introduces unphysical degrees of freedom which either cancel because of gauge invariance (QED) or are explicitly removed by including the ghost diagrams (QCD). An alternative is to work with a physical gauge in which no spurious polarisations are introduced. An example of a gauge fixing term which yields a physical gauge is,

$$\mathcal{L}_{\text{gauge-fixing}} = -\frac{1}{2\lambda}(n \cdot \mathcal{A})^2. \qquad (1.52)$$

The resulting gauge is called the axial gauge. In this gauge the two point function for the gluon field is given by,

$$\Gamma^{(2)}_{\{AB,\,\alpha\beta\}}(p) = i\delta_{AB}\left[p^2 g_{\alpha\beta} - p_\alpha p_\beta + \frac{1}{\lambda} n_\alpha n_\beta\right]. \qquad (1.53)$$

Note that in axial gauges, ghosts are not necessary. In this gauge the free propagator is given by the inverse of Eq. 1.53.

$$\Delta_{\{BC,\,\beta\gamma\}}(p)\Big|_{\text{axial}} = \delta_{BC}\frac{i}{p^2}\left[-g_{\beta\gamma} + \frac{n_\beta p_\gamma + n_\gamma p_\beta}{n \cdot p} - \frac{(n^2+\lambda p^2)}{(n\cdot p)^2} p_\beta p_\gamma\right] \qquad (1.54)$$

The axial gauge belongs to the class of physical gauges. In the following lectures we shall consider in detail the light-cone gauge $\lambda = 0$, $n^2 = 0$,

$$\Delta_{\{BC,\,\beta\gamma\}}(p)\Big|_{\text{lightcone}} = \delta_{BC}\frac{i}{p^2}\left[-g_{\beta\gamma} + \frac{n_\beta p_\gamma + n_\gamma p_\beta}{n \cdot p}\right]. \qquad (1.55)$$

This propagator corresponds to the following sum over polarisations,

$$\sum_{\text{polarisations}} \epsilon^{\alpha *}(l)\epsilon^{\beta}(l) = d^{\alpha\beta}(p) = \left(-g^{\alpha\beta} + \frac{n^{\alpha}p^{\beta} + n^{\beta}p^{\alpha}}{n \cdot p}\right). \tag{1.56}$$

Since two constraint equations are satisfied for an on-shell gluon,

$$n_{\alpha}d^{\alpha\beta}(p) = 0, \quad p_{\alpha}d^{\alpha\beta}(p) = 0 \tag{1.57}$$

there are only two physical polarisations which propagate in this gauge. For a review of physical gauges see ref. 14. The utility of physical gauges stems from the fact that they provide a closer relationship between physical intuition and the contribution of a given graph. For example, they can be used to prove theorems considering only a restricted class of graphs. The disadvantage of the axial gauge stems from the presence of the $(n \cdot p)$ singularity. For practical purposes we must find some way to regulate this singularity. In higher loops these singularities may pile up so that a consistent definition of the theory may not be possible. We shall adopt a physicist's approach and try and use the light-cone gauge as long as it does not give nonsense. In the next lecture I shall use the light cone gauge in the treatment of the QCD improved parton model.

2. LECTURE II

A. The parton model

I shall introduce the parton model by reviewing the reaction which it was invented to explain. In about 1972 a series of electron-nucleon scattering experiments

$$e^{-}(k) + H(p) \rightarrow e^{-}(k') + X \tag{2.1}$$

were performed by a SLAC-MIT collaboration[15]. A schematic diagram of this reaction is shown in Fig. 3. By measuring the energy and angle of the scattered electron one can calculate the virtuality Q^2 of the exchanged photon and the fractional energy transfer y. The lower part of the diagram in Fig. 3 describes the interaction of the virtual photon with the hadronic target and because of Lorentz

and gauge invariance has a general expansion given by,

$$W^{\mu\nu} = \left(-g^{\mu\nu} + \frac{q^\mu q^\nu}{q^2}\right) W_1(x_B, Q^2) + \left(p^\mu - \frac{\nu q^\mu}{q^2}\right)\left(p^\nu - \frac{\nu q^\nu}{q^2}\right) W_2(x_B, Q^2) \quad (2.2)$$

where μ and ν are the indices which describe the polarisations of the virtual photon. After contraction with the leptonic tensor which describes the interaction of the electron with the virtual photon we obtain the following formula for the differential cross-section.

$$\frac{d\sigma}{dx_B dy} = \frac{8\pi\alpha_{\rm em}^2}{Q^2 y}\left(\frac{y^2}{2} W_1 + (1-y)\frac{Q^2 W_2}{4x_B^2}\right) \quad (2.3)$$

$\alpha_{\rm em}$ is the electromagnetic fine-structure constant. In this formula the mass of the incoming hadron has been neglected. The SLAC-MIT experiment measured the structure functions W_1 and W_2. Before the experiments were performed it was expected that the W_1 and W_2 would fall off as a function of Q^2, like all other hadronic form-factors. In fact the experiments gave the first evidence for point-like structures in the proton since, at large Q^2 the functions F_1 and F_2 derived from W_1 and W_2 were found to be approximately independent of Q^2,

$$\begin{aligned} W_1\left(x_B, Q^2\right) &\rightarrow F_1(x_B), \\ \nu W_2\left(x_B, Q^2\right) &\rightarrow F_2(x_B). \end{aligned} \quad (2.4)$$

The derivation of this remarkable scaling result in the parton model is as follows. Assume that the virtual photon interacts with point-like constituents inside the proton. We now know that the charged consituents of the proton are quarks of spin one half, so we shall include this fact in our treatment. The hadronic tensor W can be written as

$$W^{\mu\nu}(q,p) \sim \frac{1}{4}\int d^4k \left[S^{\mu\nu}(k,q)\,\Gamma(k,p)\right] \quad (2.5)$$

where S describes the interaction of the photon with the quark, and Γ is the wave-function of the quark inside the proton as shown in Fig. 4. The dashed line indicates that the s-channel discontinuity of the diagram is taken. Both S and Γ depend on the spinor indices of the exchanged quark lines. I have suppressed these indices and introduced the notation used throughout this lecture that quantities

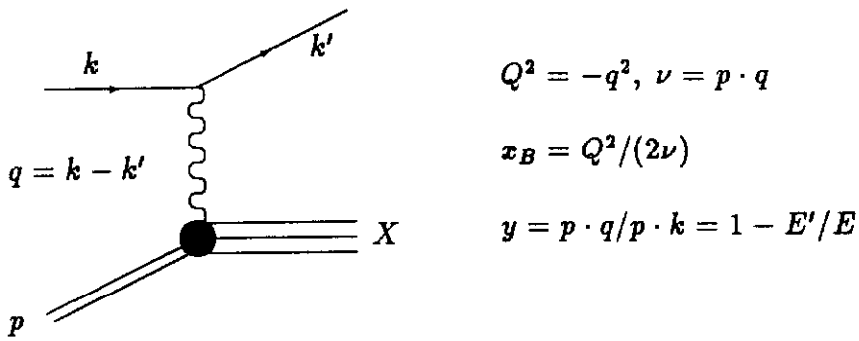

Figure 3: Deep inelastic lepton-nucleon scattering

inside square brackets are assumed to be summed over spinor indices,

$$\left[S\Gamma\right] \equiv \sum_{i,j} S_{ij}\Gamma_{ji}. \tag{2.6}$$

As a first step we perform a decomposition of the components of k, the momentum of the incoming quark line, in terms of the proton momentum p and the auxiliary vectors n and k_T.

$$k^\mu = xp^\mu + \frac{k^2 + k_T^2}{2x} n^\mu + k_T^\mu \tag{2.7}$$

By assumption we take the proton to be massless, and choose n and k_T such that the following relations are true,

$$n^2 = 0,\ p^2 = 0,\ n \cdot k_T = p \cdot k_T = 0,\ n \cdot p = 1. \tag{2.8}$$

By definition we have set $n \cdot p = 1$ so the vector n has the dimensions of an inverse mass. We first isolate the component of the momentum k collinear with the incoming momentum p,

$$W^{\mu\nu} = \frac{1}{4} \int d^4k \left[\Big(S^{\mu\nu}(xp, q) + \{ S^{\mu\nu}(k, q) - S^{\mu\nu}(xp, q) \} \Big) \Gamma(k, p) \right]. \tag{2.9}$$

We neglect for the moment the term in braces so that the expression for $W^{\mu\nu}$ becomes,

$$W^{\mu\nu}(q, p) \sim \frac{1}{4} \int dx \left[S^{\mu\nu}(xp, q)\, H(x, p, n) \right]. \tag{2.10}$$

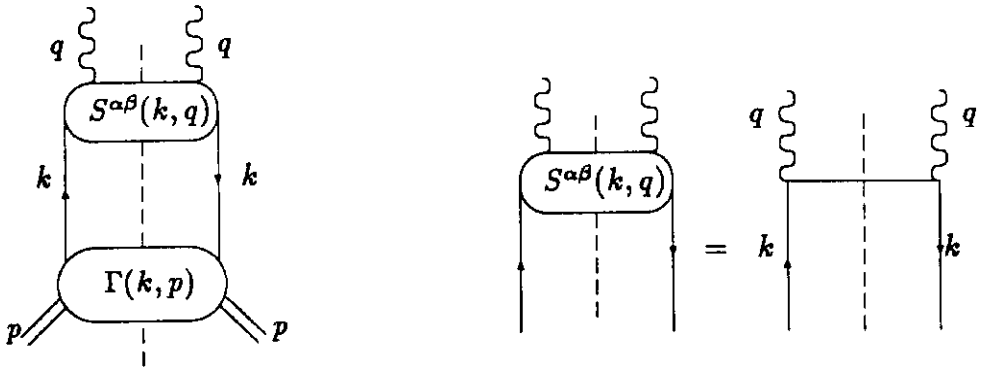

Figure 4: Deep Inelastic Scattering in the naive parton model

where H is defined as,

$$H(x,p,n) = \int d^4k\ \delta(x - n\cdot k)\Gamma\,(k,p) = \int_0^{\text{K.L.}} dk^2 dk_T^2\ \Gamma\,(k,p)\,. \tag{2.11}$$

The upper bounds on the k^2 and k_T^2 integrations are determined by kinematics. H is a spinor function which has the general expansion,

$$H(x,p,n) = q\,(x)\,\hat{p} + h\,(x)\,\hat{n}. \tag{2.12}$$

For the purposes of our simple model we assume chiral symmetry to be a good symmetry of nature. Terms like $\hat{n}\hat{p} - \hat{p}\hat{n}$ are therefore forbidden in Eq. 2.12. If Γ falls off sufficiently fast at large k, we can replace the kinematic limit (K.L.) by infinity. q and h are therefore functions of x alone. The function $h(x)$ has the dimensions of mass squared, and will combine with a term of order $1/Q^2$ from the upper part S shown in Fig. 4. It is therefore negligible at large Q^2 and can be dropped. We project out the quark distribution by contracting with n,

$$q(x) = \frac{1}{4}\int d^4k\ \delta\,(x - n\cdot k)\,[\hat{n}\Gamma(k,p)]\,. \tag{2.13}$$

The result for the leading contribution to the structure function can be expressed in terms of the quark distribution as,

$$W^{\mu\nu} \sim \frac{1}{4}\int dx\,[S^{\mu\nu}\,(xp,q)\,\hat{p}]\,q(x). \tag{2.14}$$

The model for the upper part S corresponds to a photon interacting with a free parton as shown in Fig. 4,

$$\frac{1}{4}\left[S^{\mu\nu}\left(xp,q\right)\hat{p}\right]=\frac{e_q^2}{4}\left[\gamma^\nu\left(x\hat{p}+\hat{q}\right)\gamma^\mu\hat{p}\right]\delta\left(\left(xp+q\right)^2\right). \tag{2.15}$$

e_q is the charge of the quark. Performing the trace over the spinor indices we obtain,

$$\frac{1}{4}\left[S^{\mu\nu}\left(xp,q\right)\hat{p}\right]=\frac{e_q^2}{2\nu}\left\{\left(xp^\nu+q^\nu\right)p^\mu+\left(xp^\mu+q^\mu\right)p^\nu-\nu g^{\mu\nu}\right\}\delta(x-x_B) \tag{2.16}$$

Comparing with Eq. 2.2 we find (for a single species of quark),

$$W_1=\frac{e_q^2}{2}q\left(x_B\right),\ \ \nu W_2=e_q^2x_Bq\left(x_B\right). \tag{2.17}$$

In this model the structure functions satisfy the Callan-Gross relation,

$$2x_BF_1(x_B)-F_2(x_B)=0 \tag{2.18}$$

which is a consequence of the spin one half nature of the constituents.

We now dispose of the term which we dropped from Eq. 2.9. By assumption the wave-function of the proton falls off very rapidly with k^2,k_T^2. Calling the scale which characterises that fall-off Λ it is easy to show that the terms which we dropped are of order Λ^2. Since the structure function is dimensionless they must combine with terms of order $1/Q^2$. For the same reason graphs other than the one shown in Fig. 4 can be neglected. For a systematic treatment of the $1/Q^2$ terms in parton language see ref. 16.

Deep inelastic scattering provides an example of the use of the parton model[17] in the description of hard scattering processes. In the parton model the cross-section for a process is given by the integral of the rescaled parton cross-section multiplied by the probability f_i to find a parton with a fraction x of the incoming hadron's energy.

$$\sigma^H\left(|q|,p\right)=\sum_i\int dx\ \ \sigma^P\left(|q|,xp\right)f_i(x) \tag{2.19}$$

$|q|$ stands for a large momentum scale which is necessary in order that the impulse approximation make sense, and which forbids the process to occur by the interaction of partons with a very small fraction of the longitudinal momentum of the

incoming hadron. Such parton are called wee partons. For the particular case of DIS this becomes

$$W_2 \sim \int dx\, \delta\left(2xp\cdot q - Q^2\right) q(x) \tag{2.20}$$

The identification of the quark distribution $q(x)$ defined in Eq. 2.13 with a number density of quarks with a fraction between x and $x+dx$ of the longitudinal momentum of the incoming hadron only occurs in the infinite momentum frame. A necessary condition for the concept of a number density to be sensible is that the measurement of the parton number should be instantaneous compared with the time scale of the interactions between partons. By boosting to a Lorentz frame in which the proton is moving very fast the interactions of the constituents are slowed by time dilation. In such a frame the vector p becomes very large, and hence n becomes very small. The magnitude of the components of any vector along n, such as in Eq. 2.7, are

$$\frac{k^2+k_T^2}{2x}|n|. \tag{2.21}$$

As p goes to infinity these terms, which play the role of energies[18], tend to zero, as long as x remains finite. These energies control the rate of time evolution of the parton system so it is necessary that they should vanish in order that the parton number density should have a meaning. The parton model will not be valid for processes in which arbitrarily wee partons can participate.

B. The QCD improved parton model

The simple parton model described above is not true in QCD, because the properties which we assumed for the hadronic blob Γ are explicitly violated by certain classes of graphs in perturbation theory. Nevertheless much of the structure of the parton model remains in perturbation theory, because of the property of factorisation. Factorisation permits scattering amplitudes with incoming high energy hadrons to be written as a product of a hard scattering piece and a remainder factor which contains the physics of low energies and momenta. The former contains only high energy and momentum components and, because of asymptotic freedom, is calculable in perturbation theory. The latter piece describes non-perturbative physics, but is described by a single process independent function for each type of parton called the parton distribution function. Without this property of factorisa-

tion we would be unable to make predictions for processes involving hadrons using perturbation theory.

The factorisation has been proved within perturbation theory, but it is assumed to have a validity which transcends perturbation theory. The proofs [19,20,21,22,23] require a detailed examination of all the dangerous regions of phase space in Feynman graphs.

The plausibility of the factorisation property can be seen from the following argument. The presence of infra-red singularities or singularities coming from regions of collinear emission reveals the sensitivity of a Feynman graph to very low momentum scales. Because of the Landau rules[24] such singularities are associated with real physical processes rather than virtual processes which occur only as short-lived fluctuations. Because these real processes occur long before the hard interaction it is appropriate that they are included in the wave function of the incoming hadron and not in the short distance cross-section. The proofs of factorisation establish that this simple picture is in fact valid in perturbation theory.

In QCD the graphs which contain singularities depend on the gauge chosen for the exchanged gluon. The clearest physical explanation occurs in the light cone gauge, in which the graphs responsible are the generalised ladder graphs of the type shown in Fig. 5. The rungs of the ladder K are defined to be two particle irreducible. This means that all places in which Fig. 5 can be divided into two pieces by cutting only two lines are shown explicitly as the sides of the ladder.

To show that factorisation is correct it is necessary to demonstrate, (a) that the singularities of all Feynman diagrams contributing to a given hard process can be cast in a factorisable form and (b) that the singular pieces depend only on the type of the incoming parton leg and not on the particular hard process. It is clearly a great advantage in demonstrating property (a) to have to consider only ladder graphs in which there is already a separation between the hard process and the gluon dressing coming from the rungs of the ladder. The second property (b) ensures that a parton distribution measured in one process can be used in any other hard process.

Assuming the property of factorisation to hold we can derive the QCD improved

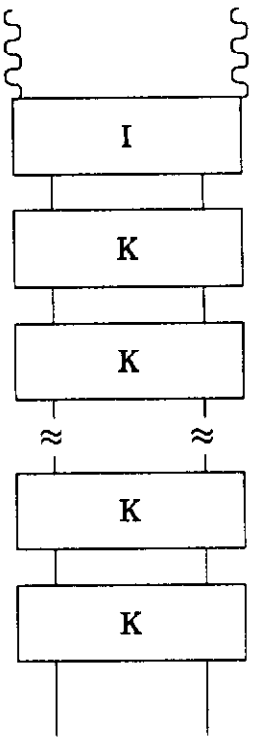

Figure 5: General ladder diagram

parton model. The result for any process with a single incoming hadron leg is,

$$\sigma^H\left(|q|,p\right)=\sum_i dx\ \sigma_i^p\left(|q|,xp,\alpha_S(\mu^2)\right)\ f_i(x,\mu^2) \tag{2.22}$$

μ^2 is the large momentum scale which characterises the hardness of the interaction. The sum i runs over all partons in the incoming hadron. σ^p is the short distance cross-section calculable as a perturbation series in the QCD coupling α_S. It is referred to as the short distance cross-section because the singularities corresponding to long distance physics have been factored out and absorbed in the structure functions f_i. The structure functions themselves are not calculable in perturbation theory. In order to perform the factorisation we have introduced a scale μ^2 which separates the high and low momentum physics. No physical results can depend on the particular value chosen for this scale. Consequently the variations of the parton distributions with changes of the scale scale μ are predicted by the Altarelli-Parisi equation[25],

$$\frac{d}{d\ln\mu^2}f_i\left(x,\mu^2\right)=\frac{\alpha_S(\mu^2)}{2\pi}\sum_j\int_0^1 dy\ dz\ \delta(x-yz)P_{ij}\left(y,\alpha_S(\mu^2)\right)\ f_j(z,\mu^2). \tag{2.23}$$

The matrix P is the Altarelli-Parisi function calculable as a perturbation series

$$P_{ij}\left(x,\alpha_S\right)=P_{ij}^{(0)}(x)+\frac{\alpha_S}{2\pi}P_{ij}^{(1)}(x)+\cdots \tag{2.24}$$

The physical interpretation of the parton distribution functions $f_j(x,\mu^2)$ again relies on the infinite momentum frame. In this frame $f_j(x,\mu^2)$ is the number of partons of type j carrying a fraction x of the longitudinal momentum of the incoming hadron and having a transverse dimension $r<1/\mu$. As we increase μ, the Altarelli-Parisi equation predicts that the number of partons will increase. Viewed on a smaller scale of transverse dimension r', such that $r'\ll 1/\mu$, a single parton of transverse dimension $1/\mu$ is resolved into a greater number of partons.

C. Factorisation in lowest order

In this section I illustrate the way that factorisation works in lowest order. Consider the simplest deep inelastic scattering graphs in which only one gluon is emitted. In the light cone gauge the only graph which contains a singularity is the ladder

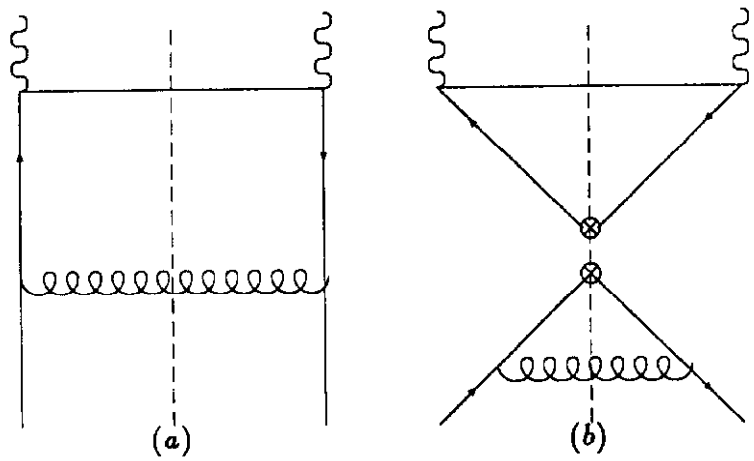

Figure 6: Factorisation in lowest order

graph with one rung shown in Fig. 6. This property can be demonstrated by a power counting argument[19] based on the properties of the quark-gluon emission vertex.

The physics of the argument can be understood as follows. Consider an incoming quark which emits a spin one gluon. Since the quark-gluon vertex is proportional to γ^α the helicity of the quark line must be conserved. Consequently the amplitude for gluon emission must vanish in the forward direction when the transverse momentum of the emitted gluon k_T tends to zero because of angular momentum conservation. In fact the amplitude vanishes as one power of k_T. This factor in the numerator is sufficient to make all graphs finite except for the ladder graph, which contains two singular denominators. The divergence in the matrix element squared for the ladder graph is of the form,

$$\frac{k_T^2}{k^4} \sim \frac{1}{k_T^2} \tag{2.25}$$

Note the importance of the spin of the gluon for this argument. In covariant gauges, such as the Feynman gauge, longitudinal gluons propagate in individual graphs, and invalidate the above argument. It is only after summing all graphs, including those where the gluon is attached to the struck quark line, that the light cone gauge result is recovered. Gauge invariance means that the choice of gauge must ultimately be irrelevant, but in physical gauges there is a simpler physical

description. In covariant gauges we lose the physical picture of the singularities being due to collinear gluon emission from incoming legs.

We restrict our attention to the deep inelastic scattering graph where the gluon emission occurs before the interaction with the virtual photon. We use a physical gauge specified by the light-like vector n. We shall regulate the singularities of Feynman graphs by working in d dimensions. This procedure, which was proposed for the regulation of ultra-violet divergences, can equally well be used for the regulation of infra-red divergences. As usual we introduce the scale μ to keep the coupling constant dimensionless in d dimensions. The one gluon emission amplitude is given by,

$$M^{\mu} \sim g\mu^{\epsilon}\bar{u}(p')\gamma^{\mu}\frac{\hat{k}}{k^2}\gamma^{\alpha}t^{A}u(p)\epsilon_{\alpha}^{A} \tag{2.26}$$

where α and A are the spin and colour indices of the emitted gluon and $p' = k + q$ is the momentum of the outgoing quark. Squaring the amplitude and performing the sum over the transverse polarisations of the emitted gluon by contracting with $d_{\alpha\beta}$ (cf. Eq. 1.56) we obtain,

$$|M^2|^{\mu\nu} \sim g^2 C_F \mu^{2\epsilon} d_{\alpha\beta}(l)\frac{1}{k^4}\left[\hat{k}\gamma^{\alpha}\hat{p}\gamma^{\beta}\hat{k}\gamma^{\nu}\hat{p}'\gamma^{\mu}\right]. \tag{2.27}$$

In this equation we have performed an average over the colour degrees of freedom of the incoming lines. The phase space of the emitted gluon in d dimensions is,

$$(PS) = \int \frac{d^d l}{(2\pi)^d} 2\pi\delta^+(l^2)(2\pi)^d\delta^d(p-k-l) \equiv 2\pi\delta^+((p-k)^2). \tag{2.28}$$

The rung of the ladder shown in Fig.7(a) can be written as,

$$K = 2\pi g^2 C_F \mu^{2\epsilon}\left(\frac{\hat{k}}{k^2}\gamma^{\alpha}\right)_{\gamma\delta}\left(\frac{\hat{k}}{k^2}\gamma^{\beta}\right)_{\gamma'\delta'}\delta^+\left((p-k)^2\right)d_{\alpha\beta}(p-k). \tag{2.29}$$

In Eq. 2.29 the colours of the incoming (outgoing) lines have been averaged (summed). Including the spin sum from the lower part of the graph we have,

$$K\hat{p}\big] = 2\pi g^2 C_F \mu^{2\epsilon}\frac{1}{k^4}\left(\hat{k}\gamma^{\alpha}\hat{p}\gamma^{\beta}\hat{k}\right)_{\gamma\gamma'}\delta^+\left((p-k)^2\right)d_{\alpha\beta}(p-k). \tag{2.30}$$

The single square bracket indicates the contraction over the $\delta\delta'$ indices. The upper and lower parts of the diagram in Fig. 6 are linked by the integration over the

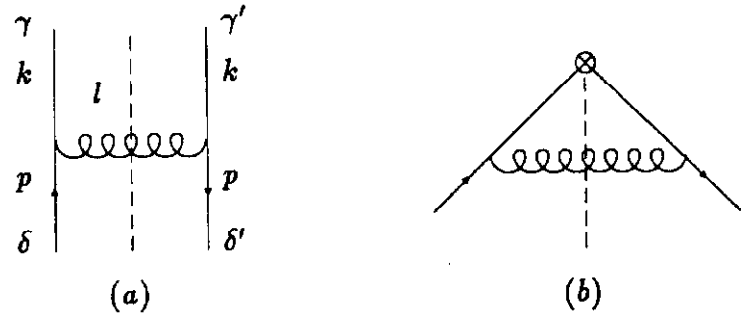

Figure 7: The quark-quark kernel

momentum k and by the contraction of the spinor indices.

$$|M^2|^{\mu\nu} \sim \int \frac{d^d k}{(2\pi)^d} \Big[C^{\mu\nu}(q,k) K\hat{p} \Big]. \tag{2.31}$$

$K\hat{p}\Big]$ has the general spinor expansion,

$$K\hat{p}\,] = \frac{1}{k^4} \left\{ A\hat{k}_{||} + B\hat{k}_T + C\hat{n}k^2 + D\hat{n}\hat{k}_T\hat{k}_{||} \right\}. \tag{2.32}$$

$k_{||} = xp$ is the component of k along the vector p. Since n has the dimensions of an inverse mass, A, B, C and D are dimensionless functions. They are also finite in the limit $k^2 \to 0$. In d dimensions the integrations over the legs of the ladder can be written in terms of the components defined in Eq. 2.7 as,

$$\int \frac{d^d k}{(2\pi)^d} = \frac{1}{(2\pi)^d} \int \frac{dx}{2|x|} dk^2 d^{d-2} k_T. \tag{2.33}$$

After integration over all angles using Eq. 1.23 this becomes

$$\int \frac{d^d k}{(2\pi)^d} = \frac{1}{32\pi^3} \frac{1}{\Gamma(1-\epsilon)} \int \frac{dx}{|x|} dk^2 dk_T^2 \left(\frac{4\pi}{k_T^2} \right)^{\epsilon}. \tag{2.34}$$

The result for the structure function including gluon emission can be schematically written as,

$$|M^2|^{\mu\nu} \sim \int \frac{dx}{x} \int_0^{q^2} \frac{dk^2}{k^2} \int_0^{-k^2(1-x)} \frac{dk_T^2}{k^2} \left(\frac{4\pi\mu^2}{k_T^2} \right)^{\epsilon} \left[\left\{ A\hat{k}_{||} + \cdots \right\} \gamma^{\nu} \hat{p}' \gamma^{\mu} \cdots \right]. \tag{2.35}$$

The upper limit on the k^2 integration is some large invariant, which is of the order of q^2. The upper limit on the transverse momentum of the recoiling system is in general determined by the condition $(p-k)^2 \geq 0$. It is therefore of the order of k^2. For the particular case of a single emitted gluon this reduces to the condition that,

$$(p-k)^2 = -\frac{(1-x)k^2}{x} - \frac{k_T^2}{x} = 0. \tag{2.36}$$

Since $k_T \sim \sqrt{-k^2}$ only the term proportional to A contains a singularity at $k_T^2 = k^2 = 0$.

The procedure for isolating the singular part is as follows. The terms in the ladder are connected by the integration over the four momentum of the legs of the ladder and by the contraction of spinor indices. For any two terms A and B in a ladder graph we introduce a spinor projector which acts as follows,

$$\Big[AB\Big] = \Big[A\mathcal{P}_n B\Big] + \Big[A(1-\mathcal{P}_n)B\Big]. \tag{2.37}$$

The specific form of the spinor projector $\mathcal{P}$ is,

$$\mathcal{P}_n = \hat{k}_{\|}\Big]\Big[\frac{\hat{n}}{4n\cdot k} \tag{2.38}$$

The projector $\mathcal{P}_n$ isolates the piece proportional to $\hat{k}_{\|}$,

$$|M^2|^{\mu\nu} \to \int d^dk \frac{1}{4n\cdot k}\left[\hat{n}\hat{k}\gamma^\alpha\hat{p}\gamma^\beta\hat{k}\right]\frac{1}{k^4}d_{\alpha\beta}(l)\left[\hat{k}_{\|}\gamma^\nu\hat{p}'\gamma^\mu\right]\cdots \tag{2.39}$$

Since we are only interested in the singular part, which occurs at $k_T^2 = 0$, we evaluate the upper part at $k = xp$, dropping terms of order k^2 and k_T^2. We also keep only the pole part (P.P.) in the lower part. The d dimensional integral reduces to a one dimensional integral linking the upper and lower part,

$$|M^2|^{\mu\nu}_{\text{sing}} = \int \frac{dx}{x} C^{\mu\nu}(q,xp)\tilde{\Gamma}\left(x,\alpha_S,\frac{1}{\epsilon}\right). \tag{2.40}$$

This result is shown symbolically in Fig. 6b.

A more formal procedure to accomplish the same end is to introduce a second projector $\mathcal{P}_\epsilon$. The action of the projector $\mathcal{P}_\epsilon$ sets $k = xp$ in all terms to its left and

extracts the pole part in ϵ from the terms to its right. The complete factorisation is performed by the action of the two projectors,

$$\mathcal{P} = \mathcal{P}_n \otimes \mathcal{P}_\epsilon. \tag{2.41}$$

The expression for $\tilde{\Gamma}$ is then,

$$\tilde{\Gamma}\left(x, \alpha_S, \frac{1}{\epsilon}\right) = \delta(1-x) + x\text{P.P.} \int \frac{d^d k}{(2\pi)^d} \delta(x - n\cdot k) \frac{1}{4n\cdot k} [\hat{n} K \hat{p}]. \tag{2.42}$$

The explicit expression for the projected kernel is,

$$\frac{1}{4n\cdot k}[\hat{n}K\hat{p}] = g^2 C_F 2\pi\mu^{2\epsilon}\delta^+\left((p-k)^2\right)\frac{1}{4n\cdot k}\left[\hat{n}\hat{k}\gamma^\alpha\hat{p}\gamma^\beta\hat{k}\right] d^{\alpha\beta}(p-k). \tag{2.43}$$

With a little algebra we can show that,

$$\begin{aligned}
&\frac{1}{4n\cdot k}\left[\hat{n}\hat{k}\gamma^\alpha\hat{p}\gamma^\beta\hat{k}\right] d_{\alpha\beta}(p-k)\,\delta(p-k)^2 \\
&= \left(\frac{1+x^2}{1-x} - \epsilon(1-x)\right)\left(-2k^2\right)\delta\left(k_T^2 + (1-x)k^2\right).
\end{aligned} \tag{2.44}$$

with x defined as in Eq. 2.7. The trace algebra is performed in d dimensions, exploiting only the relation,

$$\gamma^\alpha\gamma^\beta + \gamma^\beta\gamma^\alpha = 2g^{\alpha\beta}. \tag{2.45}$$

Dropping irrelevant $O(\epsilon)$ terms $\tilde{\Gamma}$ becomes,

$$\begin{aligned}
&\tilde{\Gamma}\left(x, \alpha_S, \frac{1}{\epsilon}\right) = \delta(1-x) \\
&-\text{P.P.}\left\{\frac{g^2}{8\pi^4}(2\pi)C_F\int\frac{dk^2}{k^2}\int d^{d-2}k_T\left(\frac{1+x^2}{1-x}\right)\delta\left(k_T^2+(1-x)k^2\right)\right\}
\end{aligned} \tag{2.46}$$

The singularity at $k_T = 0$ is regulated in d dimensions,

$$\begin{aligned}
\tilde{\Gamma}\left(x, \alpha_S, \frac{1}{\epsilon}\right) &= \delta(1-x) - \text{P.P.}\frac{\alpha_S}{2\pi}C_F\int_0^{\sim q^2}\frac{dk_T^2}{(k_T^2)^{1+\epsilon}}\left(\frac{1+x^2}{1-x}\right) \\
&= \delta(1-x) - \frac{\alpha_S}{2\pi}\frac{1}{\epsilon}C_F\left(\frac{1+x^2}{1-x}\right).
\end{aligned} \tag{2.47}$$

This is almost the complete answer for Γ, the full $O(\alpha_S)$ singular part. The full result requires self-energy insertions on the legs of the ladder. The treatment of these graphs in the light-like axial gauge is somewhat delicate. In the light-cone gauge the self energy contains ultraviolet divergences both in the terms proportional to $\hat{p}$ and in the terms proportional to $\hat{n}$. These latter divergences require a counterterm proportional to $\hat{n}$ (not present in the original Lagrangian) and have led some authors to question the practical utility of working in such a gauge. An ad-hoc procedure for dealing with these poles is given in ref. 26. We shall finesse these problems by noting that these graphs can only contribute at $x = 1$ and determining the endpoint contribution by a physical argument. In physical predictions of the QCD improved parton model Γ is factored into the quark distribution of the incoming hadron. In order to preserve conservation of quark number we must have,

$$\int_0^1 dx\ \Gamma(x, \alpha_S, \frac{1}{\epsilon}) = 1 \tag{2.48}$$

The full answer for Γ can hence be written as

$$\Gamma\left(x, \alpha_S, \frac{1}{\epsilon}\right) = \delta(1-x) - \frac{\alpha_S}{2\pi}\frac{1}{\epsilon}\left[\frac{1+x^2}{(1-x)} - \delta(1-x)\int_0^1 dy\left(\frac{1+y^2}{1-y}\right)\right] \tag{2.49}$$

This equation is normally rewritten as a "plus" distribution defined such that for any sufficiently smooth function f,

$$\int_0^1 dx \frac{f(x)}{(1-x)_+} = \int_0^1 dx \frac{f(x) - f(1)}{(1-x)}. \tag{2.50}$$

So that the final result for Γ is

$$\Gamma\left(x, \alpha_S, \frac{1}{\epsilon}\right) = \delta(1-x) - \frac{\alpha_S}{2\pi}\frac{1}{\epsilon}P_{qq}^{(0)}(x) \tag{2.51}$$

where $P_{qq}^{(0)}$ is the lowest order quark-quark term in the Altarelli-Parisi matrix,

$$P_{qq}^{(0)}(x) = C_F\left[\frac{(1+x^2)}{(1-x)_+} + \frac{3}{2}\delta(1-x)\right]. \tag{2.52}$$

3. LECTURE III

A. Factorisation

In this lecture we shall investigate the experimental consequences of the factorisation of mass singularities in a hard hadronic process. We shall continue to use as a primary example deep inelastic scattering in which there is only one incoming hadron. The demonstration of the factorisation property is more subtle in the case in which there is more than one active hadron in the initial state and is treated in Refs. 23, 27 and 28. Because of the property of factorisation the Deep Inelastic structure functions (see Eq. 2.4) can be written in perturbation theory as,

$$F_i\left(x_B, \frac{Q^2}{\mu^2}, \alpha_S, \frac{1}{\epsilon}\right) = \int_{x_B}^1 \frac{dx}{x}\, C_i\left(\frac{x_B}{x}, \frac{Q^2}{\mu^2}, \alpha_S\right) \Gamma\left(x, \alpha_S, \frac{1}{\epsilon}\right) \tag{3.1}$$

where C_i is the short distance deep inelastic scattering cross-section corresponding to the ith structure function. By construction C_i contains no mass singularities. Γ is a process independent function depending only on the type of the incoming parton leg. It is defined to contain all mass singularities order by order. In the dimensionally regularised scheme these appear as poles in ϵ. In general the function Γ is a matrix in the space of quarks and gluons. In the example given in the previous lecture we examined only the diagonal quark-quark term. We shall continue to treat this term in detail and return to the full matrix problem only when we come to deal with the phenomenology. It is convenient to rewrite Eq. 3.1 in a form which makes the convolution structure manifest,

$$F_i\left(x_B, \frac{Q^2}{\mu^2}, \alpha_S, \frac{1}{\epsilon}\right) = \int_0^1 dx \int_0^1 dy\, \delta(x_B - xy)\, C_i\left(y, \frac{Q^2}{\mu^2}, \alpha_S\right) \Gamma_{qq}\left(x, \alpha_S, \frac{1}{\epsilon}\right). \tag{3.2}$$

Since convolutions of this form occur frequently we introduce a symbolic notation,

$$C(x) = \int_0^1 dy \int_0^1 dz\, \delta(x - yz) A(y) B(z) \equiv A \otimes B. \tag{3.3}$$

We define the moments of any function by the equation,

$$F(N) = \int_0^1 dx\ x^{N-1} F(x). \tag{3.4}$$

In moment space the convolutions of the form in Eq. 3.3 reduce to a product of moments. In particular for the structure function Eq. 3.2 we find,

$$F\left(N,\frac{Q^2}{\mu^2},\alpha_S,\frac{1}{\epsilon}\right)=C\left(N,\frac{Q^2}{\mu^2},\alpha_S\right)\Gamma_{qq}\left(N,\alpha_S,\frac{1}{\epsilon}\right). \tag{3.5}$$

In the following we shall often leave unspecified whether we are working in moment space or in the space of longitudinal momentum fractions.

We now illustrate, without proof, the form of the all orders factorisation. We assume that we are working in a gauge in which all the mass singularities are due to graphs which can be divided into two pieces by cutting two lines. We call these two particle reducible graphs. These have the form of generalised ladder graphs as shown in Fig. 5. Summing the geometric series for the ladder graphs, we may write the result for the structure function as,

$$F=I+IK+IK^2+IK^3+\ldots=I\frac{1}{(1-K)}. \tag{3.6}$$

I is a two particle irreducible hard scattering term which is free from all singularities. The kernel K is also two particle irreducible and, in the light cone gauge, free from mass-singularities. The singularities are introduced by the integrations over the sides of the ladder which are implicit in Eq. 3.6. The projection operator $\mathcal{P}$ introduced in Eq. 2.41 projects out the singular part of these integrations. We may formally rewrite Eq. 3.6 as[19,26]

$$\begin{aligned} F &= I\left\{\frac{1}{(1-(1-\mathcal{P})K-\mathcal{P}K)}\right\} \\ &= \left\{I\frac{1}{(1-(1-\mathcal{P})K)}\right\}\left\{1-\mathcal{P}\frac{K}{(1-(1-\mathcal{P})K)}\right\}^{-1} \end{aligned} \tag{3.7}$$

We identify C and Γ_{qq} with the terms in braces.

$$F=C\,\Gamma_{qq},\quad C=\left\{I\frac{1}{(1-(1-\mathcal{P})K)}\right\},\quad \Gamma_{qq}=\left\{1-\mathcal{P}\frac{K}{(1-(1-\mathcal{P})K)}\right\}^{-1} \tag{3.8}$$

The expresssions for C and Γ_{qq} are defined by their power series expansions. In the expansion for C the projector $(1-\mathcal{P})$ acts on the full term to the right.

$$C=I+I(1-\mathcal{P})K+I(1-\mathcal{P})(K(1-\mathcal{P})K)+\ldots \tag{3.9}$$

whilst,

$$\Gamma_{qq} = 1 + \mathcal{P}K + \mathcal{P}K^2 - \mathcal{P}(K\mathcal{P}K) + (\mathcal{P}K)(\mathcal{P}K) + \ldots \tag{3.10}$$

Eqs. 3.9, 3.10 provide a systematic procedure for the construction of C and Γ_{qq}. For more details and an example of the implementation of this scheme through to $O(\alpha_S^2)$ we refer the reader to Ref.(26).

B. Renormalisation group behaviour

In performing the factorisation and renormalisation we were obliged to introduce a parameter μ to keep the coupling constant dimensionless in d dimensions. μ is an arbitrary parameter and consequently, with fixed bare parameters, no physical result can depend on it. This leads to the property known as renormalisation group invariance. For an introduction to the renormalisation group as applied to hard scattering processes see Ref. 29. To exploit the renormalisation group we define the total logarithmic derivative with respect to μ,

$$\mathcal{D} = \mu\frac{d}{d\mu} \equiv \mu\frac{\partial}{\partial\mu} + \tilde{\beta}(g,\epsilon)\frac{\partial}{\partial g} \tag{3.11}$$

where $\tilde{\beta}(g,\epsilon)$ is the logarithmic derivative of the renormalised coupling at fixed bare parameters,

$$\tilde{\beta}(g,\epsilon) = \mu\frac{\partial}{\partial\mu}g\Big|_{g_0,\epsilon}. \tag{3.12}$$

In the MS scheme the relationship between the bare and renormalised parameters is

$$g = \mu^{-\epsilon}Z_g^{-1}g_0. \tag{3.13}$$

By construction, Z_g contains only pole terms and therefore has a Laurent expansion in ϵ.

$$Z_g = 1 + \sum_{i=1}^{\infty}\frac{Z_g^i}{\epsilon^i} \tag{3.14}$$

The quantities Z_g^i have perturbative expansions in the renormalised coupling. We therefore find that $\tilde{\beta}$ satisfies the equation,

$$\left[\tilde{\beta}\,(g,\epsilon) + \epsilon g + g\frac{\partial}{\partial\ln\mu}\right]Z_g = 0 \tag{3.15}$$

In the minimal subtraction scheme Z_g has no explicit μ dependence. The μ-dependence enters only through the implicit dependence of the renormalised coupling. So the μ derivative can be related to a derivative with respect to g,

$$\mu\frac{\partial}{\partial\mu}Z_g\left(g\left(g_0,\mu,\epsilon\right),\epsilon\right)=\tilde{\beta}\left(g,\epsilon\right)\frac{\partial}{\partial g}Z_g, \tag{3.16}$$

and Eq. 3.15 may be written as

$$\left[\tilde{\beta}\left(g,\epsilon\right)\frac{\partial}{\partial g}g+\epsilon g\right]Z_g=0. \tag{3.17}$$

Now $\beta(g,\epsilon)$ is finite for vanishing ϵ, so that, from Eq. 3.17 it is clear that $\tilde{\beta}(g,\epsilon)$ is at most linear in ϵ. Comparing the coefficient of the linear term in ϵ we find,

$$\tilde{\beta}(g,\epsilon)=-\epsilon g+\tilde{\beta}(g). \tag{3.18}$$

Substituting for $\tilde{\beta}$, Eq. 3.17 becomes,

$$\left[\tilde{\beta}(g)\frac{\partial}{\partial g}g-\epsilon g^2\frac{\partial}{\partial g}\right]Z_g=0. \tag{3.19}$$

By further comparing the coefficients of the term of order ϵ^0 we obtain,

$$\tilde{\beta}(g)=g^2\frac{\partial}{\partial g}Z_g^{(1)}. \tag{3.20}$$

We therefore conclude that, in the MS renormalisation scheme the beta function is determined by the simple poles in Z_g to all orders in g.

In lowest order we have that,

$$Z_g^{(1)}=-\frac{g^2}{16\pi^2}\left[\frac{11N_c-4n_fT_R}{6}\right]+\ldots \tag{3.21}$$

as given in Table 2. The result for the beta function is,

$$\tilde{\beta}(g)=\frac{-g^3}{16\pi^2}\left(\frac{11N_c-4n_fT_R}{3}\right)+O(g^5) \tag{3.22}$$

We now operate with the renormalisation group operator on the left hand side of Eq. 3.5. This is equal to zero since the perturbatively calculated structure function must be independent of the choice made for the scale μ. We find that

$$\mathcal{D}\ln F=\left[\mathcal{D}\ln C+\mathcal{D}\ln\Gamma_{qq}\right]=0. \tag{3.23}$$

We now introduce a renormalisation group quantity called the anomalous dimension γ_{qq},

$$\gamma_{qq} = \frac{1}{2}\mathcal{D}\ln\Gamma_{qq} \equiv \frac{1}{2}\tilde{\beta}(g,\epsilon)\frac{\partial}{\partial g}\ln\Gamma_{qq} \tag{3.24}$$

and obtain a renormalisation group equation for short distance cross-section C.

$$\mathcal{D}C + 2\gamma_{qq}C = 0. \tag{3.25}$$

Since γ_{qq} appears in an equation involving C and $\mathcal{D}$ which are both finite in the limit $\epsilon \to 0$, γ_{qq} is also finite in that limit. In the minimal subtraction factorisation scheme Γ_{qq} has a Laurent expansion.

$$\Gamma_{qq} = 1 + \sum_{i=1}^{\infty}\frac{\Gamma_{qq}^{(i)}}{\epsilon^i}. \tag{3.26}$$

Using arguments similar to those used for the β function we can show that the anomalous dimension is determined by the simple pole in Γ_{qq}.

$$\gamma_{qq} = -\frac{1}{2}g\frac{\partial}{\partial g}\Gamma_{qq}^{(1)}. \tag{3.27}$$

C. Solution of renormalisation group equation

In this section we derive the solution of the renormalisation group equation for C, the short distance cross-section,

$$\left[\mu\frac{\partial}{\partial\mu} + \tilde{\beta}(g)\frac{\partial}{\partial g} + 2\gamma_{qq}\right] C\left(\ln\frac{Q^2}{\mu^2}, \alpha_S\right) = 0. \tag{3.28}$$

It is convenient to work in terms of the variables $\alpha_S = g^2/4\pi$ and $t = \ln Q^2/\mu^2$. We have therefore defined the function $\beta(\alpha_S) = g\tilde{\beta}(g)/(4\pi)$. In terms of these variables the renormalisation group equation Eq. 3.28 is,

$$\left[-\frac{d}{dt} + \beta(\alpha_S)\frac{d}{d\alpha_S} + \gamma_{qq}(\alpha_S)\right] C(t,\alpha_S) = 0 \tag{3.29}$$

where the expansion of the renormalisation group functions are defined by,

$$\begin{aligned}\beta(\alpha_S) &= -b\alpha_S^2(1 + b'\alpha_S\cdots), \qquad b = \left(\frac{11N_c - 4n_fT_R}{12\pi}\right),\\ \gamma_{qq}(\alpha_S) &= -c\alpha_S + c'\alpha_S^2\cdots\end{aligned} \tag{3.30}$$

Note that b and b' are independent of the renormalisation scheme[29].

To solve Eq. 3.29 it is convenient to rewrite the equation in terms of $B(t,\alpha_S) = \ln C$.

$$\left[\frac{\partial}{\partial t} - \beta(\alpha_S)\frac{\partial}{\partial \alpha_S}\right] B\,(t,\alpha_S) = \gamma_{qq}(\alpha_S). \tag{3.31}$$

This differential equation can be solved in the standard way yielding a general solution and a particular integral. The general solution of the equation,

$$\left[\frac{\partial}{\partial t} - \beta(\alpha_S)\frac{\partial}{\partial \alpha_S}\right] B(t,\alpha_S) = 0. \tag{3.32}$$

is defined in terms of the running coupling which we denote by $\alpha(t)$. The running coupling is defined by the implicit equation,

$$t = \int_{\alpha(0)}^{\alpha(t)} \frac{dx}{\beta(x)}. \tag{3.33}$$

At the renormalisation point μ the coupling $\alpha(0) = \alpha_S$. The derivatives of $\alpha(t)$ are given by,

$$\frac{\partial \alpha(t)}{\partial t} = \beta\left(\alpha(t)\right), \quad \frac{\partial \alpha(t)}{\partial \alpha_S} = \frac{\beta(\alpha(t))}{\beta(\alpha_S)}. \tag{3.34}$$

The function B expressed in terms of $\alpha(t)$ satisfies Eq. 3.32,

$$\left[\frac{\partial}{\partial t} - \beta(\alpha_S)\frac{\partial}{\partial \alpha_S}\right] B\left(0,\alpha(t)\right) = 0. \tag{3.35}$$

Including the inhomogeneous term we find that the general solution for B is,

$$B(t,\alpha_S) = B\left(0,\alpha(t)\right) + \int_{\alpha(0)}^{\alpha(t)} dx \frac{\gamma_{qq}(x)}{\beta(x)}. \tag{3.36}$$

Hence it follows that,

$$C(t,\alpha_S) = C\left(0,\alpha\left(t\right)\right) \exp \int_{\alpha(0)}^{\alpha(t)} dx \frac{\gamma_{qq}(x)}{\beta(x)}. \tag{3.37}$$

A leading logarithmic approximation to this solution can be obtained by including the first term in the perturbative expansion of the β function, Eq. 3.30,

$$t = -\int_{\alpha(0)}^{\alpha(t)} \frac{dx}{bx^2}. \tag{3.38}$$

which yields the expression,

$$\alpha(t) = \frac{\alpha(0)}{1 + \alpha(0)bt}. \tag{3.39}$$

In the limit of large t we may write this as,

$$\alpha(t) \sim \frac{1}{b \ln Q^2/\Lambda^2} + O(1/\ln^2(Q^2)). \tag{3.40}$$

Λ is a fundamental parameter of the theory, which sets the scale for the strength of the strong interactions. However it depends on the renormalisation scheme. Note in the particular that Eq. 3.40 leaves Λ undefined, since a rescaling in Λ is of the same order as terms which have been dropped.

Restoring the dependence on the moment number N, the solution for the structure function in perturbation theory may be written,

$$F_i\left(\frac{Q^2}{\mu^2}, N, \alpha_S, \frac{1}{\epsilon}\right) = C\left(1, N, \alpha(t)\right) \exp \int_{\alpha(0)}^{\alpha(t)} dx \frac{\gamma_{qq}(x)}{\beta(x)} \Gamma_{qq}\left(N, \alpha_S, \frac{1}{\epsilon}\right) \tag{3.41}$$

D. Altarelli-Parisi equation

We now make contact between the results of perturbation theory and parton distribution functions defined within a hadron. The final result for the hadronic structure function is given by the convolution of the perturbative result with a 'bare' distribution of quarks inside a hadron, q_B. It is convenient to define a 'dressed' parton distribution function,

$$q(N,t) = \Gamma_{qq}\left(N, \alpha_S, \frac{1}{\epsilon}\right) q_B\left(N, \frac{1}{\epsilon}\right) \exp \int_{\alpha(0)}^{\alpha(t)} dx \frac{\gamma_{qq}(x)}{\beta(x)} \tag{3.42}$$

The physics of the low momentum region is certainly non-perturbative. A necessary assumption in order for the whole parton picture to make sense is that the singularities in Γ_{qq} are cancelled by singularities present in the bare quark distribution function. The 'dressed' quark distribution function is therefore a finite function. Its behaviour under changes of the scale t is,

$$\frac{dq(N,t)}{dt} = \gamma_{qq}\left(N, \alpha(t)\right) q\left(N,t\right). \tag{3.43}$$

P_{qq} is the anti-Mellin transform of γ_{qq}

$$\gamma_{qq}(N,\alpha_S) = \frac{\alpha_S}{2\pi}\int_0^1 dx x^{N-1} P_{qq}(x,\alpha_S). \tag{3.44}$$

Taking the anti-Mellin transform of the Eq. 3.43 we obtain in x space.

$$\frac{dq(x,t)}{dt} = \frac{\alpha(t)}{2\pi}\int_0^1 dy \int_0^1 dz\ \delta(x-yz) P_{qq}(z,\alpha(t)) q(y,t) \tag{3.45}$$

P_{qq} has a perturbative expansion in the running coupling,

$$P_{qq}(z,\alpha_S) = P_{qq}^{(0)}(z) + \frac{\alpha_S}{2\pi} P_{qq}^{(1)}(z) + \ldots \tag{3.46}$$

So far we have only dealt with the diagonal qq case. In general we have a matrix equation known as the Altarelli-Parisi (AP) equation.

$$\frac{d}{dt}\begin{pmatrix} q(x,t) \\ g(x,t) \end{pmatrix} = \frac{\alpha(t)}{2\pi}\int_0^1 dy \int_0^1 dz\ \delta(x-yz) \begin{pmatrix} P_{qq}(y,\alpha(t)) & P_{qg}(y,\alpha(t)) \\ P_{gq}(y,\alpha(t)) & P_{gg}(y,\alpha(t)) \end{pmatrix} \begin{pmatrix} q(z,t) \\ g(z,t) \end{pmatrix} \tag{3.47}$$

The AP kernels $P_{ij}(x)$ have an attractive physical interpretation as the probability of finding parton i in a parton of type j with a fraction x of the longitudinal momentum of the parent parton and a transverse size less than $1/Q$. The interpretation as probabilities implies that the AP kernels are positive definite for $x < 1$. They satisfy the following relations.

$$\begin{aligned} &\int_0^1 dx P_{qq}(x) = 0 \\ &\int_0^1 dx\ x\Big[P_{qq}(x) + P_{gq}(x)\Big] = 0 \\ &\int_0^1 dx\ x\Big[2n_f P_{qg}(x) + P_{gg}(x)\Big] = 0. \end{aligned} \tag{3.48}$$

These equations correspond to quark number conservation and momentum conservation in the splittings of quarks and gluons.

E. Phenomenology of the Altarelli-Parisi equation

The parton distributions are fundamental objects in the QCD improved parton model. The distribution functions themselves are not calculable in perturbation

theory, but their change with $t = \ln Q^2$ is determined by the Altarelli-Parisi (AP) equations, Eq. 3.47. The kernels of the AP equations are calculable as a power series in the strong coupling α_S. Both the lowest order terms[25] and the first correction[26] to the evolution kernels have been calculated. The lowest order approximations to the evolution kernels are given as follows,

$$\begin{aligned}
P_{qq}^{(0)}(x) &= C_F\left[\frac{1+x^2}{(1-x)_+} + \frac{3}{2}\delta(1-x)\right], \\
P_{qg}^{(0)}(x) &= T_R\left[x^2 + (1-x)^2\right], \quad T_R = \frac{n_f}{2}, \\
P_{gq}^{(0)}(x) &= C_F\left[\frac{1+(1-x)^2}{x}\right], \\
P_{gg}^{(0)}(x) &= 2N_c\left[\frac{x}{(1-x)_+} + \frac{1-x}{x} + x(1-x)\right] + \delta(1-x)\frac{(11N_c - 4n_f T_R)}{6}.
\end{aligned} \tag{3.49}$$

$P_{qq}^{(0)}$ was calculated in lecture II. The other lowest order kernels are calculable using similar methods. In the space of moments these four evolution kernels take the form

$$\begin{aligned}
\gamma_{qq}^{(0)}(N) &= C_F\left[-\frac{1}{2} + \frac{1}{N(N+1)} - 2\sum_{j=2}^{N}\frac{1}{j}\right] \\
\gamma_{qg}^{(0)}(N) &= T_R\left[\frac{(2+N+N^2)}{N(N+1)(N+2)}\right] \\
\gamma_{gq}^{(0)}(N) &= C_F\left[\frac{(2+N+N^2)}{N(N^2-1)}\right] \\
\gamma_{gg}^{(0)}(N) &= 2N_c\left[-\frac{1}{12} + \frac{1}{N(N-1)} + \frac{1}{(N+1)(N+2)} - \sum_{j=2}^{N}\frac{1}{j}\right] - \frac{2}{3}n_f T_R
\end{aligned} \tag{3.50}$$

In general the $A-P$ equation is a $(2n_f+1)$ dimensional matrix equation in the space of quarks, antiquarks and gluons. However not all of the evolution kernels are distinct so the matrix equation can be considerably simplified. Because of

charge conjugation we have that,

$$P_{qq} = P_{\bar{q}\bar{q}}, \quad P_{qg} = P_{\bar{q}g}. \tag{3.51}$$

At lowest order we have in addition the following relations,

$$P^{(0)}_{\bar{q}q} = 0, \quad P^{(0)}_{q_i q_j} = 0 \quad (i \neq j). \tag{3.52}$$

The solution of the AP equation is simplified by considering combinations which are non-singlet (in flavour space) such as $q_i - \bar{q}_i$ or $q_i - q_j$. In this combination the mixing with the flavour singlet gluons drops out and we have, $(V = q_i - q_j)$,

$$\frac{d}{dt}V(x,t) = \frac{\alpha(t)}{2\pi}\left[P_{qq}(y) \otimes V(z,t)\right]. \tag{3.53}$$

Taking moments this equation becomes,

$$\frac{dV(N,t)}{dt} = \frac{\alpha(t)}{2\pi}\gamma_{qq}(N)\, V(N,t). \tag{3.54}$$

Inserting the lowest order form for the running coupling We find the solution,

$$V(N,t) = V(N,0)\, t^{d_N} = V(N,0)\left(\frac{\alpha(0)}{\alpha(t)}\right)^{d_N}, \quad d_N = \frac{\gamma^{(0)}_{qq}(N)}{2\pi b}. \tag{3.55}$$

The parton radiation leads to a degradation of the momentum. This is evident in Eq. 3.55 because $\gamma_{qq}(N) < 0$ and the moments shrink as t tends to infinity.

We now turn to the flavour singlet combination of moments. Define the sum over all quark flavours to be given by Σ,

$$\Sigma = \sum_i q_i + \bar{q}_i. \tag{3.56}$$

From Eq. 3.47, which holds for all flavours of quarks, we derive the equation for the flavour singlet combination of parton distributions,

$$\begin{aligned}
\frac{d\Sigma}{dt} &= \frac{\alpha(t)}{2\pi}\left[P_{qq} \otimes \Sigma + 2n_f P_{qg} \otimes g\right] + 0\left(\alpha^2(t)\right) \\
\frac{dg}{dt} &= \frac{\alpha(t)}{2\pi}\left[P_{gq} \otimes \Sigma + P_{gg} \otimes g\right] + 0\left(\alpha^2(t)\right)
\end{aligned} \tag{3.57}$$

This equation is most easily resolved by direct numerical integration in x space starting with an input distribution obtained from data. This has been done by many authors and parametrisations of the solutions are available in the literature[30,31,32].

We will only illustrate a few simple properties by taking moments. Taking the second ($N = 2$) moment of the Eq. 3.57 we find that.

$$\frac{d}{dt}\begin{pmatrix}\Sigma(2)\\ g(2)\end{pmatrix} = \frac{\alpha(t)}{2\pi}\begin{pmatrix}-C_F\frac{4}{3} & \frac{n_f}{3}\\ C_F\frac{4}{3} & \frac{-n_f}{3}\end{pmatrix}\begin{pmatrix}\Sigma(2)\\ g(2)\end{pmatrix} \tag{3.58}$$

The eigenvectors and corresponding eigenvalues of this system of equations are,

$$\begin{aligned} O^+(2) &= \Sigma(2) + g(2) \quad \text{Eigenvalue : } 0 \\ O^-(2) &= \Sigma(2) - \frac{n_f}{4C_F}g(2) \quad \text{Eigenvalue : } -\left(\frac{4}{3}C_F + \frac{n_f}{3}\right). \end{aligned} \tag{3.59}$$

Note that the combination O^+, which corresponds to the total momentum carried by the quarks is independent of t. The eigenvector O^- vanishes at asymptotic t.

$$O^-(2) = \left(\frac{\alpha(0)}{\alpha(t)}\right)^{-\frac{\left(\frac{4}{3}C_F+\frac{n_f}{3}\right)}{2\pi b}}. \tag{3.60}$$

So that asymptotically we have that,

$$\frac{\Sigma(2)}{g(2)} = \frac{n_f}{4C_F} = \frac{N_c n_f}{2(N_c^2-1)}. \tag{3.61}$$

The momentum fractions carried asymptotically by the quarks and gluons are given by,

$$\Sigma(2)\Big|_{t=\infty} = \left(\frac{n_f}{4C_F+n_f}\right), \quad g(2)\Big|_{t=\infty} = \left(\frac{4C_F}{4C_F+n_f}\right) \tag{3.62}$$

Note however that the approach to the asymptotic limit is controlled by $t \sim \ln Q^2$ and is therefore quite slow. For a tabulation of the eigenvectors and eigenvalues of for general N we refer the reader to Ref. 3.

The gluon distribution grows rapidly at small x. We shall now give an analytic estimate of the rate of growth of the gluon distribution function. When $\ln(1/x)$ is large the one loop evolution equations are dominated by the poles at $x = 0$ which appear in the AP splitting functions,

$$P_{gg}(x) \to \frac{2N_c}{x}, \quad P_{gq}(x) \to \frac{2C_F}{x}. \tag{3.63}$$

The small x behaviour of the gluon distribution is driven by P_{gg}. Denoting the momentum distribution of the gluons by $G(x,t) = xg(x,t)$ we obtain from the AP equation that,

$$\frac{dG(x,t)}{dt} = \frac{\alpha(t)N_c}{\pi}\int_x^1 \frac{dz}{z}G(z,t) \tag{3.64}$$

Making the changes of variables,

$$\xi = b\int^t dt'\alpha(t'), \quad y = \frac{2N_c}{\pi b}\ln(1/x), \tag{3.65}$$

Eq, 3.64 can be cast in the form,

$$\frac{d^2G(y,\xi)}{d\xi dy} = \frac{1}{2}G(y,\xi). \tag{3.66}$$

At large ξy the solution to this equation is,

$$G(y,\xi) \sim \exp(\sqrt{2\xi y}), \tag{3.67}$$

which expressed in the original variables yields,

$$g(x) \sim \frac{1}{x}\exp\sqrt{\frac{4N_c}{\pi b}\ln\frac{\ln Q^2/\Lambda^2}{\ln Q_0^2/\Lambda^2}\ln\frac{1}{x}}, \quad N_c = 3, \quad b = \frac{(33-2n_f)}{12\pi}. \tag{3.68}$$

A topic which is presently under active investigation[33] is the mechanism which limits the growth of the gluon distribution. In the infinite momentum frame the gluon momentum distribution $G(x,t)$ gives the number of gluons per unit of rapidity with a transverse size less than $1/Q$. If the number of gluons grows so large that the partons start to jostle one another new effects will come into play. A crude estimate of when this begins to happen is provided by,

$$G(x,t) = \frac{\text{Area of hadron}}{\text{Area of parton}} \sim Q^2r^2 \sim 25Q^2\text{GeV}^{-2}. \tag{3.69}$$

where $r \sim 1/m_\pi$ is the radius of the hadron. At presently attainable values of x the value of $G(x,\ln(Q^2))$ does not exceed 3 or 4, so the saturation limit is beyond the range of the present colliders.

4. LECTURE IV

A. Fragmentation functions

The methods of the QCD improved parton model can also be applied to the decay of a parton. In this case it is appropriate to define a decay function D_i^H which describes the fragmentation of a parton i into a hadron H which carries a fraction z of the longitudinal momentum of the incoming parton. These fragmentation functions are most easily extracted from e^+e^- annihilation. If q is the timelike four momentum of the virtual photon, $q^2 = Q^2$, we find that the pion inclusive cross-section may be written as

$$\frac{d\sigma}{dz} = 3\sigma_0 \sum_f e_f^2 \left[D_q^\pi(z,t) + D_{\bar{q}}^\pi(z,t) \right], \tag{4.1}$$

$$z = \frac{2p \cdot q}{Q^2}, \quad t = \ln \frac{Q^2}{\Lambda^2}. \tag{4.2}$$

σ_0 is the cross-section for the production of a single colour of quark antiquark pair. In magnitude it is equal to the muon pair production cross section. Because of the effects of collinear radiation the fragmentation functions satisfy the timelike modification of the Altarelli-Parisi equation,

$$\begin{aligned} \frac{d}{dt} D_q(z,t) &= \frac{\alpha_S(t)}{2\pi} \left[D_q^\pi \otimes P_{qq} + D_g^\pi \otimes P_{gq} \right] \\ \frac{d}{dt} D_g(z,t) &= \frac{\alpha_S(t)}{2\pi} \left[\left(D_q^\pi + D_{\bar{q}}^\pi \right) \otimes P_{qg} + D_g^\pi \otimes P_{gg} \right]. \end{aligned} \tag{4.3}$$

In the leading logarithmic approximation, (lowest order in α_S), the A-P kernels are the same as for the space-like parton distribution case. The first corrections to the timelike A-P kernels are given in Ref. 26. Corrections to the short-distance cross-section are discussed in Ref. 34.

Note that the multiplicity of hadrons in the final state is given by,

$$\sum_H \int dz \frac{d\sigma}{dz} = < n^H > \sigma_{tot} \tag{4.4}$$

The total multiplicity is related to the first moment of the fragmentation function.

B. Multiplicities in jets

An important problem for the design of experimental detectors is the multiplicity of hadrons to be expected in a high energy jet. A high energy jet can be thought of as a highly virtual timelike parton which decreases its virtuality by parton bremsstrahlung leading to a parton shower. At some low virtuality the methods of perturbation theory cease to be valid and the partons fragment into hadrons. In QCD the hadron multiplicity of a gluon jet is not perturbatively calculable because this last phase of jet evolution is not described by perturbation theory. However the growth of the multiplicity with the energy of the jet is determined by the parton shower and is a reliable prediction of perturbative QCD. We take as our starting point the AP evolution equation for the gluon fragmentation function.

$$\frac{d}{dt}D_g(N,t) = \frac{\alpha_S(t)}{2\pi}\left[D_g(N)\gamma_{gg}(N) + \ldots\right]. \tag{4.5}$$

The driving term is the growth of the multiplicity of the gluons so we neglect the effects of mixing with quarks. From Eq. 3.50 the anomalous dimension corresponding to the gluon splitting function contains a singularity for $N = 1$. Retaining only this most singular term we see that,

$$\frac{dD_g(N,t)}{dt} \sim \frac{\alpha_S}{2\pi}\frac{2N_c}{(N-1)}D_g(N,t). \tag{4.6}$$

The singularity at $N = 1$ is due to the emission of soft gluons. Because of this singularity it would appear at first sight that the growth of the multiplicity is not calculable in QCD.

This is not correct. The energy dependence of the multiplicity is calculable because of an interplay of kinematic and dynamic effects as we shall now demonstrate. Remember that the AP equation in lowest order corresponds to a summation of ladder diagrams with each rung containing a single gluon exchange.

In x space we may write the AP equation as,

$$\frac{dD_g(Q^2,\mu^2,x)}{d\ln Q^2} = \frac{\alpha_S(\ln Q^2)}{2\pi}\int_x^1 \frac{dz}{z}P(z)D_g\left(Q^2,\mu^2,\frac{x}{z}\right) \tag{4.7}$$

where $D_g(Q^2,\mu^2,x)$ is the fragmentation function of a gluon of all virtualities up to scale Q^2. μ^2 is some lower cut-off at which the fragmentation becomes

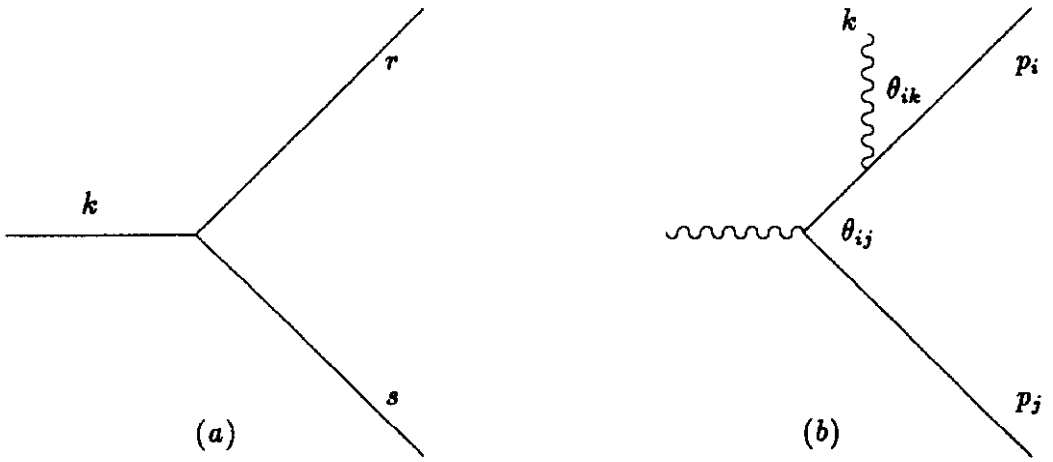

Figure 8: (a) Kinematics of parton cascade. (b) Angular ordering in QED

non-perturbative. Let us introduce the function $d(r^2,\mu^2,x)$ which describes the fragmentation of gluons of virtuality r^2.

$$D_g\left(Q^2,\mu^2,x\right)=\int_{\mu^2}^{Q^2}\frac{dr^2}{r^2}d\left(r^2,\mu^2,x\right) \tag{4.8}$$

In terms of d the AP equation can be rewritten as,

$$d\left(k^2,\mu^2,x\right)\sim\int_x^1\frac{dz}{z}P(z)\int_{\mu^2}^{k^2}\frac{dr^2}{r^2}\frac{\alpha_S(\ln r^2)}{2\pi}d\left(r^2,\mu^2,\frac{x}{z}\right) \tag{4.9}$$

In Eq. 4.9 we have dropped a homogeneous term which vanishes for $k^2\gg\mu^2$. In this form the ladder structure of the equation is manifest. Since we are interested in the emission of very soft gluons it is important to consider the kinematics of the gluon splitting in detail. A gluon of momentum k splits into two gluons of momenta r and s as shown in Fig. 8(a). We now introduce the Sudakov decompositions for k,r and s.

$$k^\mu=p^\mu+\frac{k_T^2}{2}n^\mu,\quad r^\mu=zp^\mu+\frac{r^2+r_T^2}{2z}n^\mu+r_T^\mu,\quad s^\mu=(1-z)p^\mu+\frac{s^2+r_T^2}{2(1-z)}n^\mu-r_T^\mu \tag{4.10}$$

The maximum value of r^2 comes from the region $r_T^2=s^2=0$ and is given by

$$zk^2>r^2 \tag{4.11}$$

Correctly including this kinematic constraint Eq. 4.9 becomes,

$$d\left(k^2,\mu^2,x\right) \sim \int_x^1 \frac{dz}{z} P(z) \int_{\mu^2}^{k^2 z} \frac{dr^2}{r^2} \frac{\alpha_S(\ln r^2)}{2\pi} d\left(r^2,\mu^2,\frac{x}{z}\right) \tag{4.12}$$

In terms of the original fragmentation function D_g this can be written as,

$$k^2 \frac{\partial}{\partial k^2} D_g\left(k^2,x\right) \sim \frac{\alpha(\ln k^2)}{2\pi} \int_x^1 \frac{dz}{z} \frac{2N_c}{z} D_g\left(k^2 z,\frac{x}{z}\right) \tag{4.13}$$

Note that the rescaling of $k^2 \to k^2 z$ would be non-leading were it not for the singularity of P_{gg} at $z = 0$. For simplicity we first consider the case of a fixed coupling constant, defined as $\tilde{\alpha} = N_c \alpha_S/\pi$. Taking moments of Eq. 4.13 we obtain,

$$\frac{d}{d\ln k^2} D_g(N,k^2) = \tilde{\alpha} \int_0^1 \frac{dz}{z} z^{N-1} D_g(N, zk^2). \tag{4.14}$$

If D_g has the anomalous dimension $\gamma(N)$, then $D_g(N) \sim (k^2)^{\gamma(N)}$. With this ansatz D_g satisfies,

$$\left[\frac{d}{d\ln k^2} - \gamma(N)\right] D_g(N) = 0 \tag{4.15}$$

and γ is given by,

$$\gamma(N) = \frac{\tilde{\alpha}}{N - 1 + \gamma(N)}. \tag{4.16}$$

We obtain the following answer for γ.

$$\gamma(N) = -\frac{(N-1)}{2} \pm \sqrt{\left(\frac{(N-1)^2}{4} + \tilde{\alpha}\right)} = \frac{\tilde{\alpha}}{(N-1)} - \frac{\tilde{\alpha}^2}{(N-1)^3} + \ldots \tag{4.17}$$

Note that the resummed $\gamma(N)$ is finite for $N = 1$ although every term in the power series expansion is infinite. The emission of very soft gluons has been inhibited by kinematics and the divergence at $N = 1$ has been tamed.

Eq 4.17 is still the wrong answer for the anomalous dimension in QCD, because for very soft gluons it is not sufficient to consider only the ladder graphs which are included in the AP equation. The Altarelli-Parisi equation treats correctly all logarithms of Q^2 but not all logs of $1/x$. Interference graphs are as important as ladder graphs. Remarkably it turns out in explicit calculation[4,36] that the net effect of the interference graphs is to remove all the contributions of the ladder graphs in all regions in which the emission angles are not ordered down the cascade.

The correct answer in QCD is given by the ladder graphs with a dynamical constraint that the gluons are emitted at ever decreasing angles as we proceed to lower virtualities. The result for $\gamma(N)$ is,

$$\gamma(N) = -\frac{(N-1)}{4} + \sqrt{\frac{(N-1)^2}{16} + \frac{\tilde{\alpha}}{2}} = \frac{\tilde{\alpha}}{(N-1)} - \frac{2\tilde{\alpha}^2}{(N-1)^3} + \ldots \tag{4.18}$$

Solving Eq. 4.5 we obtain,

$$D_g(Q^2, N) \sim \exp \int^{\ln Q^2} \gamma_N \left(\bar{\alpha}_S(t)\right) dt \tag{4.19}$$

which for the first moment gives,

$$D_g(Q^2, N=1) \sim \exp \int^{\ln Q^2} \sqrt{\frac{N_c}{2\pi b t}} dt \sim \exp\, 2\sqrt{\frac{N_c}{2\pi b} \ln Q^2/\mu^2} \tag{4.20}$$

A heuristic explanation of the reason for angular ordering can be obtained[38] by using an analogy from QED. Consider an incoming virtual photon which decays into an electron-positron pair as shown in Fig. 8(b). An additional soft photon of momentum k is subsequently radiated from the electron-positron pair. The virtual state consisting of an electron and a positron differs in energy from the final state containing an electron, a positron and a soft photon by an energy ΔE,

$$\begin{aligned} \Delta E &= (E_i + E_j + E_k) - (E_{i+k} + E_j) \\ &= \sqrt{|\vec{p}_i|^2 + m^2} + |\vec{k}| - \sqrt{\left(\vec{p}_i + \vec{k}\right)^2 + m^2}. \end{aligned} \tag{4.21}$$

In the limit of very large $\vec{p}_i$ and small θ_{ik} this becomes,

$$\Delta E \sim |\vec{k}| \theta_{ik}^2. \tag{4.22}$$

By the uncertainty principle the virtual electron state lives for a time Δt which is approximately given by

$$\Delta t \sim \frac{1}{|\vec{k}|\theta_{ik}^2} \sim \frac{\lambda_T}{\theta_{ik}}, \tag{4.23}$$

where $\lambda_T \sim 1/k_T \sim 1/(k\theta_{ik})$ is the transverse wavelength of the emitted soft photon. In this interval of time Δt the electron and positron separate a transverse distance given by

$$\Delta d = \Delta t \theta_{ij} = \frac{\lambda_T \theta_{ij}}{\theta_{ik}}. \tag{4.24}$$

If $\theta_{ik} > \theta_{ij}$, the separation of the electron and positron is less than the transverse wavelength of the emitted soft photon. The emitted soft photon perceives the electron-positron pair as an unresolved charge neutral object and no radiation occurs. If, on the other hand, the emitted photon lies within the cone described by the electron positron pair, $\theta_{ik} > \theta_{ij}$, the radiation is uninhibited.

This example indicates the reason for angular ordering in QED. The generalisation of this argument to QCD is complicated by the fact that the gluons themselves carry colour charge, but the angular ordering result persists.

C. Vector boson production

The simplest application of the QCD improved parton model to the case where there are two hadrons in the initial state is the process,

$$\begin{aligned} H_1 + H_2 \;\rightarrow\; & \gamma^* + X \\ & \hookrightarrow \mu^+ + \mu^- \end{aligned} \tag{4.25}$$

The lowest order short distance cross-section is due to quark-antiquark annihilation as shown in Fig. 9(a). The resulting cross-section is given by,

$$\sigma = \frac{4\pi\alpha_{em}^2}{3Q^2 s}\delta(1-z), \quad z = \frac{Q^2}{s} \tag{4.26}$$

where Q^2 is mass squared of the lepton pair and s is the square of the parton centre of mass energy. Inserting this parton cross-section in the QCD improved parton model formula we obtain,

$$\begin{aligned} \frac{d\sigma}{dQ^2} \;=\; & \frac{4\pi\alpha_{em}^2}{3Q^2 S}\frac{1}{N_c}\int_0^1 \frac{dx_1}{x_1}\int_0^1 \frac{dx_2}{x_2} \\ & \times \sum_f e_f^2 \left[q^{[1]}(x_1,t)\,\bar{q}^{[2]}(x_2,t) + (1 \leftrightarrow 2)\right]\delta\left(1 - \frac{\tau}{x_1 x_2}\right) \end{aligned} \tag{4.27}$$

The factor of $1/N_c$ is necessary because the annihilating quark-antiquark pair must be in a colour singlet state. We have introduced the variable $\tau = Q^2/S$ which has simple properties under the rescaling of the incoming momenta. S is the square of the total hadron centre of mass energy and $s = x_1 x_2 S$.

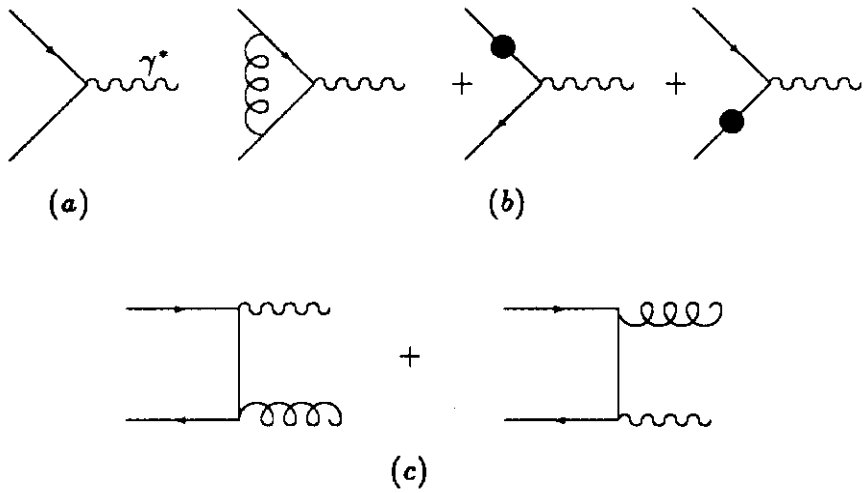

Figure 9: Feynman graphs for muon pair production

Experimentally the rapidity of the muon pair can also be measured. It is defined as,

$$y = \frac{1}{2} \ln \left(\frac{E + p_{||}}{E - p_{||}} \right) \tag{4.28}$$

where E and $p_{||}$ are the energy and longitudinal momentum of the muon pair. A measurement of both the mass and rapidity of the muon pair completely specifies the x's at which the quark distributions are probed.

$$\frac{d\sigma}{dQ^2 dy} = \frac{4\pi\alpha_{em}^2}{3Q^2 S N_c} \sum_f e_f^2 \left[q^{[1]}\left(\sqrt{\tau}e^{y}, t\right) \bar{q}^{[2]}\left(\sqrt{\tau}e^{-y}, t\right) + (1 \leftrightarrow 2) \right] \tag{4.29}$$

All input functions in Eqs. 4.27 and 4.29 are determined. The quark and anti-quark distributions are known from deep inelastic scattering. This model predicts many of the observed features of the data, such as the dependence on the nucleon number A and the angular distributions of the produced muons. For a review of experimental data on muon pair production see Ref. 43. However, at fixed target energies it is found experimentally that the cross-section for continuum muon pair production is about twice as large as predicted by Eqs. 4.27 and 4.29. In the literature this is referred to as the K-factor.

In an asymptotically free theory Eqs. 4.27 and 4.29 are the lowest order terms in a systematic expansion in the running coupling constant. The first radiative corrections to Eqs. 4.27 and 4.29 have been calculated.[40,41]. The lowest order graph is shown in Fig. 9(a). The higher order contributions are of two types. The virtual corrections are due to the inteference of the lowest order with the graphs of Fig. 9(b). The two graphs involving real gluon emission are shown in Fig. 9(c).

In calculating these diagrams we encounter mass singularities just as in the case of Deep Inelastic scattering. As before these singularities are regulated by continuing the dimension of space-time, $d = 4 - 2\epsilon$. The total cross-section is a function only of the variable $z = Q^2/s$. After dropping an overall normalisation factor the result for the full α_S result is as follows.

$$\hat{\sigma} = \delta(1-z) - \frac{\alpha_S}{2\pi} 2P_{qq}(z)\frac{1}{\epsilon} + \frac{\alpha_S}{2\pi} f_{q,DY}\left(z, \frac{Q^2}{\mu^2}\right) \tag{4.30}$$

Where $f_{q,DY}$ is a calculated function found in Ref. 40. This result can be written in a form in which the factorisable structure is manifest,

$$\hat{\sigma} = \int \frac{dx_1}{x_1}\frac{dx_2}{x_2}\left[\delta\left(1 - \frac{z}{x_1 x_2}\right) + \frac{\alpha_S}{2\pi} f_{q,DY}\left(\frac{z}{x_1 x_2}, \frac{Q^2}{\mu^2}\right)\right]$$
$$\times\left[\Gamma_{qq}(x_1, \alpha_S, \frac{1}{\epsilon})\,\Gamma_{qq}(x_2, \alpha_S, \frac{1}{\epsilon})\right] + 0\left(\alpha_S^2\right) \tag{4.31}$$

Because of the universality of the mass singularity, Γ_{qq} is given by the same expression as in Eq. 2.51.

$$\Gamma_{qq}(x, \alpha_S, \frac{1}{\epsilon}) = \left\{\delta(1-x) - \frac{1}{\epsilon}\frac{\alpha_S}{2\pi} P_{qq}(x)\right\} + 0\left(\alpha_S^2\right) \tag{4.32}$$

Eq. 4.31 should be compared with the analogous result in deep inelastic scattering. Written in similar factorised form it becomes,

$$\frac{F_2(x_B)}{x_B} = \int \frac{dx_1}{x_1}\left[\delta\left(1 - \frac{x_B}{x_1}\right) + \frac{\alpha_S}{2\pi} f_{q,2}\left(\frac{x_B}{x_1}, \frac{Q^2}{\mu^2}\right)\right]\left[\Gamma_{qq}(x_1, \alpha_S, \frac{1}{\epsilon})\right] + 0\left(\alpha_S^2\right) \tag{4.33}$$

In the MS scheme one simply absorbs Γ_{qq} into the bare quark distribution. This corresponds to a particular choice for the dressed quark distribution function.

However, Eq. 4.33 could equally well be written in the form,

$$\frac{F_2(x_B)}{x_B} = \int \frac{dx_1}{x_1}\delta\left(1-\frac{x_B}{x_1}\right)\left[\delta(1-x_1) - \frac{1}{\epsilon}\frac{\alpha_S}{2\pi}P_{qq}(x_1) + \frac{\alpha_S}{2\pi}f_{q,2}(x_1)\right] + 0\left(\alpha_S^2\right) \tag{4.34}$$

Since we actually measure quark distributions in DIS, it is useful to define a physical scheme in which the term in braces in Eq. 4.34 is absorbed into the dressed quark distribution. In this scheme[40] the measured F_2 is exactly given by the parton model formula $F_2(x_B,Q^2)/x_B = q(x_B,Q^2)$ and the corresponding Γ^P_{qq} is,

$$\Gamma^P_{qq}(x_1) = \left[\delta(1-x_1) - \frac{1}{\epsilon}\frac{\alpha_S}{2\pi}P_{qq}(x_1) + \frac{\alpha_S}{2\pi}f_{q,2}(x_1)\right] \tag{4.35}$$

In terms of these physical distribution functions, the DY cross-section is given (after physical factorisation) by,

$$\begin{aligned}\frac{d\sigma}{dQ^2} &= \int_0^1 \frac{dx_1}{x_1}\frac{dx_2}{x_2}\left[\delta\left(1-\frac{z}{x_1x_2}\right) + \frac{\alpha_S(t)}{2\pi}\left(f_{q,DY}\left(\frac{z}{x_1x_2}\right) - 2f_{q,2}\left(\frac{z}{x_1x_2}\right)\right)\right] \\ &\quad \times\left[q^{[1]}(x_1,t)\,\bar{q}^{[2]}(x_2,t) + (1\leftrightarrow 2)\right] \\ &\quad + \frac{\alpha_S(t)}{2\pi}\left(f_{g,DY}\left(\frac{z}{x_1x_2}\right) - f_{g,2}\left(\frac{z}{x_1x_2}\right)\right)\left[q^{[1]}(x_1,t)\,g^{[2]}(x_2,t) + (1\leftrightarrow 2)\right]\end{aligned} \tag{4.36}$$

Note the inclusion of the gluon-quark term. This term is due to real emission diagrams not shown in Fig. 9(c). They can be obtained from the diagrams of Fig. 9(c) by crossing an outgoing gluon and an incoming antiquark. After factorisation, these give rise to the gluon-quark terms in Eq. 4.36.

The result for the $O(\alpha_S)$ correction is,

$$\begin{aligned}\left(f_{q,DY}(z) - 2f_{q,2}(z)\right) &= C_F\Big[\frac{3}{(1-z)_+} - 6 - 4z + 2\left(1+z^2\right)\left(\frac{\ln(1-z)}{1-z}\right)_+ \\ &\quad + \left(1+\frac{4}{3}\pi^2\right)\delta(1-z)\Big] \qquad (4.37) \\ \left(f_{g,DY}(z) - f_{g,2}(z)\right) &= \frac{1}{2}\Big[\left(z^2+(1-z)^2\right)\ln(1-z) + \frac{9}{2}z^2 - 5z + \frac{3}{2}\Big]\end{aligned}$$

At fixed target energies it is found that the corrections are quite large. For example,

the value of first moment of the correction,

$$(f_{q,DY}(N=1) - 2f_{q,2}(N=1)) \sim 13. \tag{4.38}$$

This is both a triumph and an embarassment. Since the corrections are of order 100% the theory is brought into accord with the experimental number. But such a large correction casts considerable doubt on the reliability of the $O(\alpha_S)$ result. Attempts to resum the numerically most important terms present in higher orders can be found in ref. 42.

A similar formula with a different normalisation describes W and Z production. Note that for the case of vector boson production the $O(\alpha_S)$ terms give a correction of only 35%. This is mainly because the running coupling α_S is evaluated at the mass of the produced vector boson and is therefore smaller. The cross-sections for vector boson production are expected to be reliably predicted in perturbation theory. For the comparison of intermediate vector boson cross sections calculated using the Drell-Yan model with experiment, I refer the reader to 45.

D. Vector boson decay

It therefore appears that W and Z production present a better place to test the QCD improved parton model. Since the vector bosons are observed experimentally through their decays into charged leptons, reliable estimates of the leptonic branching ratios will be necessary to perform these tests. In this section we discuss the decays of the W and Z. The branching fractions into the various decay modes are determined simply by the squares of the couplings. Assuming that all final state particles are massless, the partial widths of the W's are found to be in the ratios,

$$\begin{array}{llll} \Gamma(W^- \to e^-\overline{\nu}_e) & : \Gamma(W^- \to \mu^-\overline{\nu}_\mu) & : \Gamma(W^- \to \tau^-\overline{\nu}_\tau) & : \Gamma(W^- \to q_i\overline{q}_j) \\ 1 & : 1 & : 1 & : N_c|U_{ij}|^2. \end{array} \tag{4.39}$$

U is the Kobayashi-Maskawa matrix. The factor of N_c in Eq. 4.39 takes into account the three colours of quarks. The hadronic decay mode is therefore enhanced relative to the leptonic mode. Unfortunately this decay mode of the W has a very serious background from normal QCD jet production. A first attempt to observe the hadronic decay of the W is reported in ref. 44. The decay into the mode $t\overline{b}$ is

of great interest since it offers the possibility of observing the top quark. Taking the mass of the top quark into account, (but setting the mass of the bottom quark equal to zero), the partial width of the W into top and bottom quarks is reduced from the expression given for $q_i\bar{q}_j$ above. The correct result is,

$$\Gamma(W^- \to b\bar{t}) \to N_c|U_{tb}|^2(1-r_W)(1-\frac{r_W}{2}(1+r_W)) \tag{4.40}$$

where $r_W = m_t^2/m_W^2$. Counting up all modes we see that the branching ratio into a given leptonic channel such as $e^-\overline{\nu}_e$ is,

$$\frac{1}{12} < B < \frac{1}{9} \tag{4.41}$$

The larger value holds when the decay to the top quark is forbidden.

For the Z the expressions for the branching fractions are more complicated because the couplings to the Z depend on the charge and weak hypercharge of the fermions. The result is,

$$\begin{array}{llll} \Gamma(Z^0 \to \nu_e\overline{\nu}_e) & : \Gamma(Z^0 \to e^+e^-) & : \Gamma(Z^0 \to u\bar{u}) & : \Gamma(Z^0 \to d\bar{d}) \\ 2 & : 1+(1-4x_w)^2 & : N_c(1+(1-\frac{8}{3}x_w)^2) & : N_c(1+(1-\frac{4}{3}x_w)^2) \end{array} \tag{4.42}$$

where $x_w = \sin^2\theta_w$.

The effect of the mass of the top quark is very significant in this case. Including the effect of the top quark in both the matrix element and the phase space we find that,

$$\Gamma(Z^0 \to t\bar{t}) \to N_c\sqrt{1-4r_Z}\left[1+(1-\frac{8}{3}x_w)^2+2r_Z((1-\frac{8}{3}x_w)^2-2)\right] \tag{4.43}$$

where $r_Z = m_t^2/m_Z^2$

A measurement of the width of the Z would provide useful information on the mass of the top quark and the number of massless neutrinos. At a hadron collider the width of the Z is hard to measure directly, so we consider an indirect method, which however requires a greater amount of theoretical input. The method expresses the ratio R of the number of observed W and Z decays as follows,

$$R = \frac{\text{Number of decays } W \to e\nu}{\text{Number of decays } Z \to ee} = \frac{\sigma_W}{\sigma_Z} \cdot \frac{\text{BR}(W \to e\nu)}{\text{BR}(Z \to ee)} = R_\sigma \cdot R_{\text{BR}}. \tag{4.44}$$

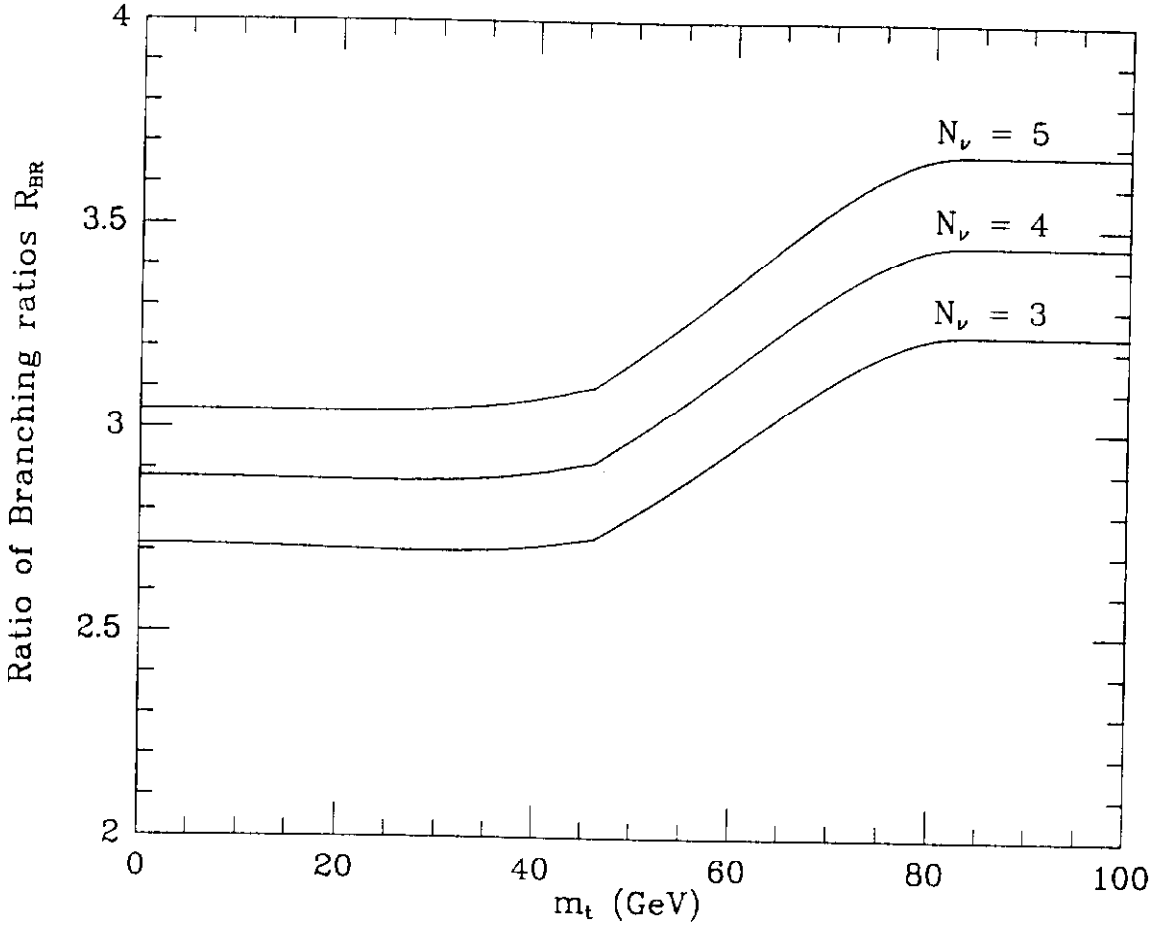

Figure 10: The ratio of the W and Z branching ratios R_{BR}.

If we know the masses of all the charged objects to which the W decays we can calculate the branching ratio for the decay of the W into electron-neutrino. Together with the theoretical value for the ratio of the cross-sections, we obtain information on the branching ratio of the Z. The ratio R_σ is calculable theoretically, with a certain error due to ignorance of the input structure functions. Unfortunately we do not know the mass of the top quark, so the limit on the mass of the top quark is correlated with the limit on the number of neutrinos. This shown in Fig. 10 where the ratio of the branching ratios is plotted as a function of the top quark mass. Experimental data rule out a large value for N_ν. In a less certain way they also provide an upper bound on the mass of the top quark, which is more stringent for a larger number of neutrinos. For $N_\nu = 3$ the bound[46] on the top quark mass is $m_t < 63$ GeV. If the mass of the top quark is so large that the decay into the W is forbidden no limit can be obtained.

Acknowledgement.

The written version of these lectures was completed at the Institute for Theoretical Physics of the University of Santa Barbara. The research was supported in part by the National Science Foundation under grant No. PHY82-17853, supplemented by funds from the National Aeronautics and Space Administration.

References

[1] Bjorken and Drell, 'Relativistic Quantum Fields', McGraw Hill, New York (1964).

[2] C. Itzykson and J. B. Zuber, 'Quantum Field Theory', McGraw Hill, New York (1980).

[3] G. Altarelli, *Phys. Rep.* **81** (1982) 1 .

[4] A. H. Mueller, *Phys. Rep.* **73** (1981) 237 .

[5] A. H. Mueller, TASI 1985.

[6] I. Hinchliffe, TASI 1986.

[7] E. Abers and B. W. Lee, *Phys. Rep.* **9** (1973) 1 .

[8] L. Faddeev and V. N. Popov, *Phys. Lett.* **258** (1977) 377 .

[9] G. t'Hooft and M. J. G. Veltman, Diagrammar, Cern Yellow Report 73-9. published in the proceedings of the summer schoool, 'Particle Interactions At Very High Energies, Part B', Louvain 1973.

[10] J. C. Collins, 'Renormalisation', Cambridge University Press, Cambridge (1984).

[11] G. t'Hooft and M. J. G. Veltman, *Nucl. Phys.* **B44** (1972) 189 ;
G. G. Bollini and J. J. Giambiagi, *Nuovo Cimento* **12B** (1972) 20 ;
W. J. Marciano, *Phys. Rev. D***12** (1975) 3861 .

[12] R. P. Feynman, Proceedings of the 1976 'Les Houches' summer school, R. Balian and C. H. Llewellyn Smith, (eds.).

[13] For a demonstration of Cutkosky rules for a one loop self-energy diagram see E. M. Lifshitz and L. P. Pitaevskii, 'Relativistic Quantum Theory', Pergamon Press (1973).

[14] G. Leibbrandt, *Rev. Mod. Phys.* **59** (1987) 4 .

[15] J. I. Friedman and H. W. Kendall, *Ann. Rev. Nucl. Part. Sci.* **22** (1972) 203 :
G. Miller *et al.*, *Phys. Rev. D***5** (1972) 528 .

[16] R. K. Ellis, W. Furmanski and R. Petronzio, *Nucl. Phys.* **B207** (1982) 1 .

[17] R. P. Feynman, 'Photon Hadron Interactions', W.A. Benjamin, New York (1972).

[18] J. Kogut and L. Susskind, *Phys. Rep.* **C8** (1973) 76 .

[19] R. K. Ellis *et al.*, *Nucl. Phys.* **B152** (1979) 285 .

[20] A. H. Mueller, *Phys. Rev. D***18** (1978) 3705 .

[21] D. Amati *et al. Nucl. Phys.* **B140** (1978) 54 .

[22] A. Efremov and A. Radyushkin, *Theor. Math. Phys.* **44** (1981) 664 .

[23] J. C. Collins *et al.*, *Phys. Lett.* **109B** (1982) 388 ;
Nucl. Phys. **B223** (1983) 381 ;
Phys. Lett. **134B** (1984) 263 .

[24] see, for example, R. J. Eden, P. V. Landshoff, D. Olive and J. C. Polkinghorne, 'The Analytic S-Matrix', Cambridge University Press, Cambridge (1066).

[25] G. Altarelli and G. Parisi, *Nucl. Phys.* **B126** (1977) 298

[26] G. Curci, W. Furmanski and R. Petronzio, *Nucl. Phys.* **B175** (1980) 27 .

[27] W. Lindsay *et al. Nucl. Phys.* **B214** (1983) 61

[28] J. Frenkel *et al. Nucl. Phys.* **B223** (1984) 307

[29] D. J. Gross, Proceedings of the 1975 Les Houches summer school, 'Methods in Field theory' ed. R. Balian and J. Zinn-Justin.

[30] D. Duke and J. F. Owens, *Phys. Rev. D***30** (1984) 49 .

[31] E. J. Eichten, K. D. Lane, I. Hinchliffe and C. Quigg, *Rev. Mod. Phys.* **56** (1984) 579 , (E:58, (1986) 1065).

[32] M. Diemoz, F. Ferroni, E. Longo and G. Martinelli, CERN-TH-4751/87 (1987).

[33] L. Gribov, E. Levin and M. Ryskin, *Phys. Rep.* **100** (1983) 1 .

[34] G. Altarelli *et al.*, *Nucl. Phys.* **B160** (1979) 301

[35] A. H. Mueller, *Phys. Lett.* **104B** (1981) 161 , *Nucl. Phys.* **B213** (1983) 85 , *Nucl. Phys.* **B241** (1984) 141 .

[36] A. Bassetto, M. Ciafaloni , G. Marchesini and A. H. Mueller, *Nucl. Phys.* **B207** (1982) 189 .

[37] Yu. L. Dokshitzer, V. A. Khoze and S. I. Troyan, Leningrad preprint 1218 (1986).

[38] Yu. L. Dokshitzer, V. A. Khoze, S. I. Troyan and A. H. Mueller, Columbia preprint CU-TP-374 (1987).

[39] Ya. I. Azimov, Yu. L. Dokshitzer, V. A. Khoze and S. I. Troyan, *Sov. J. Nucl. Phys.* **43** (1986) 95 .

[40] G. Altarelli, R. K. Ellis and G. Martinelli, *Nucl. Phys.* **B147** (1979) 461

[41] J. Kubar-Andre and F. E. Paige, *Phys. Rev. D***19** (1979) 221 .

[42] G. Parisi, *Phys. Lett.* **90B** (1980) 295 ;
G. Curci and M. Greco, *Phys. Lett.* **92B** (1980) 175

[43] I. Kenyon, *Rep. Prog. Phys.* 45 (1982) 1261.

[44] R. Ansari *et al.*, *Phys. Lett.* **B186** (1987) 452 .

[45] G. Altarelli, Proceedings of the 23rd International Conference on High Energy Physics, Berkeley, 1986.

[46] A. D. Martin *et al.*, *Phys. Lett.* **B189** (1987) 220 .